UNIVERSITY OF CALIFORNIA

Los Angeles

ALKALINE HYDROLYSIS OF TNT -
MODELING MASS TRANSPORT EFFECT

A dissertation submitted in partial satisfaction of the

requirements for the degree Doctor of Philosophy

in Civil Engineering

by

Yi-Ching Wu

2001

The dissertation of Yi-Ching Wu is approved.

_____

Thomas C. Harmon

_____

Keith D. Stolzenbach

_____

Irwin H. Suffet

_____

Michael K. Stenstrom, Committee Chair

University of California, Los Angeles

2001

*To all the people I love*

# TABLE OF CONTENTS

# LIST OF FIGURES

**Figure    Description**

## LIST OF FIGURES (CONTINUED)

**Figure     Description**

# LIST OF TABLES

**Table        Description**

# ACKNOWLEDGEMENTS

It is the most difficult part in this dissertation.

Too many people I need to thank for. Too much appreciation I have to express.

I am so afraid that I may omit anyone who helped me in my study process. So, I will try to remember all of them. And in this short paragraph, I just want to say: "thank you for your kind support."

First, of course, I have to thank for my professor, Michael Stenstrom. I still remember when I bravely yet nervously talked to him and asked him to admit me to UCLA. Without him, I might have given up studying. He is not only my professor but also my benefactor.

I need to thank Professor Stolzenbach for helping me understand the physical modeling of my simulation. I learned a lot from him. Professor Harmon and Professor Suffet helped me both in class taking and diffusion coefficient correction. Professor Yen and Dr. Chou of National Taiwan University gave me the chance to study the diffusion mechanism, the basic knowledge of the diaphragm cell and diffusion coefficient cell design. Professor Sun taught me the finite difference method.

I also want to thank Ed Ruth who helped me build the diffusion cell and the glass shop in Chemistry Dept. to make it. I wish to thank Sim-Lin for helping me in the laboratory and measuring the KCl concentration with IC.  I wish to thank Jennifer who taught me how to do RDX experiments and David for measuring the TNT reaction coefficients, and Bobby for helping with the detailed literature review. Peter helped to

debug the Matlab programs. Thanks to Ko, Mike, Andy and Chien-hou for both academic and friendly support.

I cannot forget to thank my family and friends giving me the best support. My father, of course, I should devote this Ph. D to you. My sisters, Bell and Elaine, although you often made trouble for me, I am so happy to live with you.

Finally I want to thank all my friends, Shanching, Yihyin and little Gue; they are my good friends and I always feel your standing beside me. Yi-cheng inspireds me in many aspects. Lunchang helped both in emotional and living aspects, without him I would be difficult to finish my Masters degree. Steve, without his information, I wouldn't know how  to transfer to UCLA.

I may not remember all of the people who ever helped me during the study process, but I would like to thank all of you. Thank you, with my deepest heart.

# VITA

| | |
|---|---|
| Apr 03, 1973 | Born in Tainan, Taiwan |
| 1995 | Bachelor of Science |
| | Department of Chemical Engineering |
| | National Taiwan University, Taiwan |
| 1996-1997 | Master of Science |
| | Department of Civil and Environmental Engineering |
| | University of California, Los Angeles |
| 1997-2001 | Research Assistant |
| | Department of Civil and Environmental Engineering |
| | University of California, Los Angeles |

## ABSTRACT OF THE DISSERTATION

ALKALINE HYDROLYSIS OF TNT -
MODELING MASS TRANSPORT EFFECT


by


Yi-Ching Wu

Doctor of Philosophy in Civil Engineering

University of California, Los Angeles, 2001

Professor Michael K. Stenstrom, Chair



TNT was the most widely used explosive and during the two World Wars, many countries produced million tons of TNT. After the end of the Cold War, many countries had excess inventory of weapons that contain TNT.  TNT is a challenging problem to treat for safety reasons as well as its low biodegradability.  TNT is a reported mutagen and carcinogen and also cause damage to humans who inhale it.

Several treatment techniques for TNT are reviewed. Biological treatment such as composting, bioslurry and in-situ biodegradation are highly desirable, but have had mixed success, with toxic intermediates or unknown by-products.  Physico chemical

methods for destroying TNT are more expensive but may be more reliable. Alkaline hydrolysis has been successfully used for non-aromatic explosives such as RDX and HMX but has not generally been evaluated for TNT.

The dissertation focuses on the mathematical modeling of treating particulate TNT using alkaline hydrolysis. Several modeling assumptions were evaluated. TNT diffusion coefficients were experimentally measured and compared to classical methods to predict diffusion coefficients.. The measured diffusivities and reaction rates were used to model TNT destruction for single particles as well as for collections of different sized particles. Diffusion and dissolution of TNT appear to be the rate-limiting step in the proposed treatment of TNT by alkaline hydrolysis. Experimental verification in a facility capable of handling modest amounts of TNT should be performed next.

# CHAPTER 1

# INTRODUCTION

## 1.1 Introduction

During the two World Wars many countries produced million of tons of explosives.

Many of these explosives were stock piled for future use, but with the end of the cold war,

they were no longer needed. Therefore there is a continuing need for the environmentally

safe methods for disposing of explosives.  In the past open burning (OB) or open

detonation (OD) was widely used. Both methods are very safe for workers and minimize

the chance of unwanted detonations, but these methods are no longer used due to noise,

toxic residues in local soils, and air pollution from incomplete combustion or by-product

formation.  Problems with contamination from explosives still exist at munitions,

production, storage and disposal facilities but also in areas affected by military activity.

Military bases and many industrial areas in the United States and Europe are contaminated

with explosives residues.

TNT (2,4,6-Trinitrotoluene), a nitroaromatic compound was previously the most

widely used explosive worldwide.  It is a component of bombs, artillery shells, torpedoes,

mines and even nuclear weapons. Although TNT in no longer manufactured in the United

States, it continues to be of very high interest and a potential disposal problem at certain US

Department of Energy (DOE) sites (USDHS, 1995).

TNT contaminated waters contain only relatively small concentrations due to its low

solubility (101.5 mg/L at 25°C).  The amount can still be significant when compared to

toxicity levels to fish of 1.6 mg/L (96 hr $LC_{50}$; Yinon, 1990).  Therefore treatment

technologies for wastewaters or contaminated soils are usually different than treatment

technologies for bulk explosives.  It may be possible to combine bulk treatment methods

with other processes, such as carbon adsorption.  Adsorption onto activated carbon is a

common method for treating wastewaters and contaminated groundwaters.  This in effect

creates a bulk disposal problem from a dilute TNT source, since the TNT-laden carbon is

classified as an explosive waste.

The susceptibility of 2,4,6-Trinitrotoluene (TNT) to nucleophilic attack has been well

documented (Hantzsch and Kissel, 1899).  Nucleophilic attach occurs during alkaline

hydrolysis of TNT.  This property is currently being used as a way to transform TNT into

non-energetic compounds.  Recent studies have been conducted in Germany (Saupe *et al*,

1996) and at Los Alamos National Laboratory (Spontarelli *et al*, 1996) and in our laboratory (Prisley *et al,* 1997). Many of the kinetic parameters used in this study were originally measured by Prisley.

The objectives of this research are to understand the potential mass transfer limitations of alkaline hydrolysis of TNT.  A commercial process for destroying TNT would probably use high pH (~ 11 to 12) process waters to destroy TNT particles.  The mass transfer rates of OH$^-$ and TNT to and from the particle surfaces could likely be the rate-limiting step.  To understand the mass transfer steps, the molecular diffusivity of TNT was determine and a model was developed to simulate alkaline hydrolysis.  Several different assumptions for reaction and mass transfer conditions were evaluated. Recommendations for future research are also made.

# CHAPTER 2

# LITERATURE REVIEW

## 2.1 Introduction

TNT was discovered by Wilbrand in 1863, when he added toluene to a mixture of

nitric and sulfuric acids and produced a yellow, odorless needle-like solid. The German

military began to using TNT for military applications in 1902 (Yinon, 1990). During the

two World Wars, many countries produced millions of tons TNT for use in binary

explosives (Yinon, 1990). TNT was the most important and widely used military high

explosive until well after the end of World War II. It was also used for industrial purposes

including underwater blasting, mining and as a chemical intermediate in the manufacture

of photographic chemicals and dye. TNT production was banned in the United States in the

1980s due to the lack of adequate treatment and disposal methods. Significant

environmental problems arose from the manufacture of TNT. All US production facilities

have been closed (Tsai, 1991) and as of this writing (2001), TNT is only produced in

mainland China.

## 2.2 Physical and Chemical Properties

TNT is a yellow odorless needle-shaped crystal. Figure 2.1 shows its chemical structure. It has a molecular weight of 227.15 and is sparingly soluble in water. TNT is generally available in three different grades, which are characterized by melting point. The highest purity TNT has the highest melting point of 80.65°C (Urbanski, 1964). Solubility is approximately 130 mg/L (Urbanski, 1964) at 20°C. TNT has a specific gravity of 1.6. Table 2.1 lists physical and chemical properties of TNT (USDHS, 1995).

TNT can crystallize in both monoclinic and orthorhombic polymorphic forms. The two forms have different molecular packing. The two configurations have conformationally unique molecules A and B. The basic unit is composed of 4 asymmetric parings of molecules (Gallagher, et al., 1997). The monoclinic structure has an AABBAABB packing motif while the orthorhombic structure adopts an ABABABAB packing motif. The monoclinic form is yellow colored and is more stable than the orthorhombic form. The monoclinic form is used almost exclusively in explosives. Figure 2.2 shows the molecular forms of A and B in monoclinic structure.

## 2.3 Toxicity and Environmental Fate

TNT was reported to cause health effects such as liver damage, anemia, respiratory complications, and aplastic anemia at $1.5mg/m^3$ air concentration (USDHS, 1995). TNT can be absorbed through the skin (The Merck Index, 11th edition). It is toxic to rats, mice, unicellular green algae, copepods, and oysters. Concentrations above 2 mg/L are toxic to certain fish (Osmon and Klausmeier, 1972). TNT inhibits the growth of many fungi, yeasts, actinomycetes, and gram-positive bacteria (Kaplan and Kaplan, 1982), as well as exhibiting mutagenicity in the Ames screening test (USDHS, 1995). TNT in water shows toxicity to aquatic organisms and mammals at 60 mg/L and 44 mg/L, respectively. Aerobic microbial treatment of TNT creates degradation products of 1,3,5-trinitrobenzene, 2,4-dinitrotolulene (2,4-DNT), and 2,6-dinitrotolulene (2,6-DNT). The DNT isomers are listed by the USEPA as possible carcinogens (USEPA, 1980).

TNT is persistent in surface waters due to its low vapor pressure of $1.99 \times 10^{-4}$ mmHg and solubility of 130mg/L at $20^{o}$C (USDHS, 1995). It is generally not stripped from raw and neutralized wastewater samples. A volatilization half–life of 119 days was determined in 1-meter depth river at $20^{o}$C (USDHS, 1995.)

TNT has a soil-organic carbon adsorption coefficient (Koc) of 300-1100 and will not

significantly partition from surface waters to sediments, or strongly sorb to soil particles.

This was established in short-term laboratory adsorption/desorption tests and long-term

studies. The average adsorption coefficient Kd, for all soils testes has a value of 4 units

(USDHS, 1995), which also indicates limited sorption ability. Adsorption was consistently

lower under oxidizing conditions than under reducing conditions. Most of the TNT

adsorbed was desorbed after multiple water extractions of the test soils.  The pH did not

affect TNT adsorption/desorption or transformation. Crystalline TNT persists in soils and

exists as chunks of weathered crystals, or tiny crystals embedded in the soil matrix, or as

TNT molecules adsorbed on the soil surface (Ro, et al., 1996).

 The low Kow values of 2.2-2.7 suggests that TNT will not bioconcentrate to high

levels (concentrations >100 times in media concentration) in the tissue of exposed plants

and animals or biomagnify in terrestrial aquatic food chains. Limited bioconcentration was

found in aquatic bioassays with water fleas (*Daphnia Magna*), worms, algae, and blue gill

sunfish.  Bioconcentration factors (BCFs) in 96-hour static tests were 209 for the water

fleas, 202 for worms, 453 for algae, 9.5 for fish muscle, and 338 for fish viscera.

 TNT is released to the atmosphere when open detonation or open burning techniques

are used to demilitarize munitions.  TNT in the atmosphere is degraded by direct photolysis.

The half-life for photooxidation of TNT in the atmosphere ranges from18.4 to 184 days.

The half –life ranges from 3.7-11.3 hours in distilled water (USDHS, 1995).  TNT can be

transformed in surface water by microbial metabolism even through this process is slower

than photolysis. The predicted biodegradation half-life of TNT in surface water ranges

from 1 to 6 months.

**2.4 Treatment Technologies**

**2.4.1 Biological Treatment**

Biological treatment of TNT and its by-products continues to be of high interests. The

effectiveness of this method is highly dependent on the adaptability and survival of the

microorganisms performing the degradation (Tsai, 1991).  The literature is filled with

conflicting results.

Kaplan (1992) found no significant mineralization and only partial transformation of

TNT, with an  accumulation of amino derivatives and polymerized or conjugated products.

Many species of bacteria, yeast, and fungi reduce the nitro groups to amines or azoxy

dimers but stop short of any mineralization of the aromatic ring.

Composting has been recognized as a potential treatment of hazardous wastes.

Composting of TNT requires constant oxygen supply, moisture and temperature. Previous

work suggest that,65% can be transformed within 10 weeks (Ojha, 1997). Under both

mesophilic (35-40°C) and thermophilic (55-60°C) conditions, TNT concentrations were

reduced by 98% and 99.6% for mesophilic and thermophilic piles, respectively.

Composting may generate toxic by-products or unknown end-products which also

contaminate soils.

Bioslurry treatment is an engineering arrangement of other more widely used

biotreatment approaches, including land farming and composting. It is also easy to scale up.

Bioslurry treatment is similar to other biotreatment processes with microbiological

interactions and containment pathways. The degradation rate of bioslurry treatment can be

increased by increasing the availability of contaminant, electron acceptors, nutrients and

other microbiological consortia (Zappi, et al. 1994). It is necessary to maintain oxygen

concentration by diffusing air into the slurry because oxygen uptake rates are often higher

than 20 mg/L-hr.  Aerobic mineralization of 25% of the initial TNT was reported over 11

weeks with acetate as co-metabolite and surfactants as desorption agent.

A new process, the J. R. Simplot Ex-Situ bioremediation Technology, also named as

the J. R. Simplot Anaerobia Bioremediation Procress (SA-BRE[TM]) is currently being

marketed to bioremeidate TNT. It claims to anaerobically degrade nitroaromatic

compounds with total destruction of toxic intermediate compounds (Jackson and Hunter,

1995). The Simplot process is initiated under aerobic conditions which change to quickly

become anaerobic and enable the selected microbes to degrade TNT and its toxic

intermediate compounds. This technique was tested at the Weldon Spring Ordnance Works

(WSOW) treating TNT contaminated soils and reached reduction efficiency as high as

99.4% in 9 months. The diffusion of TNT from solid-phase to liquid-phase appears to be

rate-limiting step (Jackson and Hunter, 1995). High temperature must be maintained to

promote biological activity.

   In-situ biodegradation treatment is being used at many contaminated sites. This

technique treats the waste at the local site with the native microbial community. In-situ

bioremediation systems can simple and inexpensive. Field tests show that additional

carbon sources increase $CO_2$ production but inhibit TNT mineralization. Bradley and

Chapelle, (1995) reported complete degradation of TNT in surface soil using in-situ

biodegradation treatment over 22 days.

   The various reported studies show conflicting results. This probably results because

of the inability to document mineralization and measure end-products. The effectiveness of

in-situ treatment is difficult to verify because it is almost impossible to perform a mass

balance before and after treatment in soils. Since TNT is a controlled substance and special

facilities are required to safely conduct research, few well controlled laboratory studies

exists.  Much of the evidence for TNT biodegradation is anecdotal, being observed at

munitions facilities as opposed to being measured in well-controlled experiments.

## 2.4.2 Open Burning/Open Detonation (OB/OD)

Open burning (OB) or open detonation (OD) is widely practiced due to the safety

from unwanted denotations (USDHS, 1995). OB/OD is cost-effective and it was the best

"first-generation" technology. Open burning operates as self-sustained combustion ignited

by an external source, such as flame or detonation wave. By contrast, open detonation

destroys explosives and munitions with a detonation initiated by a disposable charge. It

was reported that 80% of the US Department of Defense's (DOD) annual demilitarization

tonnage of 56,000 metric tons was destroyed using this technology in 1992. OB/OD is

affected by location and weather. The operations can be performed only under suitable

weather conditions, because wind may transport toxic fumes to neighborhood and rain will

severely affect ignition. OB/OD is becoming more difficult due to regulatory resistance,

and may soon be prohibited due to environmental and legal concerns (USDHS, 1995).

### 2.4.3 Incineration

Incineration is used to treat explosives-contaminated soil and debris as well as wastes with a mixture of media and bulk explosives. Incineration is a "second-generation" technology, which still has problems with application. The process transforms or mineralizes the hazardous material, but leaves nearly equivalent amounts of incinerated soil or ash (Major and Amos, 1992). It was originally thought that incineration could replace OB/OD as a treatment method for the disposal of high explosives. This generally has not occurred due to transportation cost of explosives or explosives-contaminated soils. Incineration may also cause serious air pollution and generates noise emission as in OB/OD. In addition, the ash from incineration also requires disposal.

### 2.4.4 Activated Carbon Adsorption

Activated carbon adsorption has proved effective in the treatment of explosives-contaminated wastewaters and has been widely used. It efficiently removes TNT from aqueous and gaseous waste streams. Granular activated carbon (GAC) systems are used in many US Army munitions plants to treat pink or red water. Pink water or red

water is a wastewater from TNT manufacturing, loading or packing, which can contain

TNT or by products. Isotherm testing must be performed to determine the relative GAC

adsorption ability, capacity and the exhaustion rate.

Although TNT can be effectively removed from the wastewater by GAC adsorption,

the laden GAC becomes a waste disposal problem. The exhausted carbon is still hazardous,

and concerns exist over the safety of its storage and transportation. Conventional thermal

regeneration cannot be applied because explosion occurs when the explosives content

exceeds 80 mg explosive/g activated carbon. Activated carbon loadings of 200 - 250 mg

explosive/g activated carbon are easily achieved (Heilmann and Stenstrom, 1996). Large

amounts of adsorbent are required if loading rates are restricted. The exhausted activated

carbon is a hazardous waste and must be isolated or thermally regenerated after a single use

(Heilmann and Stenstrom, 1996). Additionally, commercial regenerators often do not want

to regenerate explosives-laden carbon due to safety concerns, or unwillingness to mix the

carbon with carbon from other sources, such as drinking water treatment plants. If the

carbons are mixed, the regenerated carbon from a munitions plant may be reused in a

drinking water treatment plant.

### 2.4.5 Ultraviolet Radiation

UV oxidation, unlike carbon treatment, does not transfer or concentrate target compounds in another form. UV oxidation can be applied to treat wastewater from the demilitarization of munitions and for groundwater contaminated from the disposal of these waters. However, UV radiation is not very efficient for large-scale treatment processes. Also it cannot be used to treat contaminated soils. Ryon, et al. (1984) found that exposure of TNT and its associated compounds to UV radiation results in degradation of the parent compound, which suggests that the effluent is safe for disposal. When hydrogen peroxide is also present, an unstable intermediate has been documented which will be eventually be mineralized to carbon dioxide and ammonia. Analytical results show the destruction of the intermediate product 1,3,5-TNB is rate controlling. It may be necessary to use additional treatment with GAC to remove 1,3,5-TNB (Anyanwu *et al*. 1993).

### 2.4.6 Alkaline Hydrolysis

Alkaline hydrolysis has been known as a disposal method for various explosives since World War II. In the early 1980's, the US military examined the process for treating TNT-contaminated soils and sediments. Several studies have been performed in our

laboratory using alkaline hydrolysis to destroy explosives (Heilmann *et al,* 1996). The background, theory and other details will be discussed later.

Investigators at the Los Alamos National Laboratory (Spontarelli *et al* 1993) have recently investigated alkaline hydrolysis for explosives destruction. The study focused primarily on HMX (Octahydro-1,3,5,7-tetranitro-1,3,5,7-tetrazocine) explosive, but it was also reported that TNT is degraded to a non-energetic substance. The base hydrolysis of TNT produces a very dark, water-soluble product, which has not yet been identified.  They also suggested that the hydrolysates can be thermally treated using supercritical water oxidation to mineralize and produce more readily degradable products (Spontarelli, et. al., 1993).

A recent joint study conducted by the Fraunhofer IITB - Aussenstelle fuer Prozessoptimierung Berlin, BC Berlin - Consult GmbH, and the Analytisches Zentrum Berlin-Adlershof evaluated alkaline hydrolysis of TNT as a process for remediating contaminated soils.  Using NaOH as the base (1.4 g TNT/g NaOH), they found that TNT was fully and irreversibly transformed within four hours at temperatures ranging from 60 - 100 °C  to non-energetic substances (Fraunhofer *et al*, 1995).  As with other studies, a comprehensive analysis of the deep black hydrolysate was not conducted.  Further

treatment was achieved by heating the hydrolysate to temperatures ranging from 150 - 350 °C, with best results at temperatures above 200 °C. A solid was separated and the remaining liquid was then treated both anaerobically and aerobically. Attempts to degrade the hydrolysate biologically (without thermal treatment) were unsuccessful; however, denitrification was observed when a co-substrate was added (Fraunhofer *et al*, 1995).

At 80 °C, the hydrolysis of TNT results in partial mineralization (Saupe *et al,* 1996). At least one mole of nitrite per mole of TNT was found in the hydrolysate. Additionally, carbonate (10% of the TNT-C as inorganic C) and small amounts of ammonium were identified. Microfiltration of the hydrolysate showed that 60% of the products had molecular weights in excess of 30 kDa.
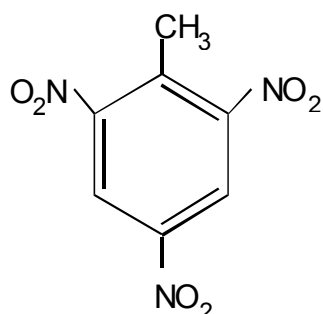
Figure 2.1: Chemical Structure of TNT (From USDHS, 1995)



A

B
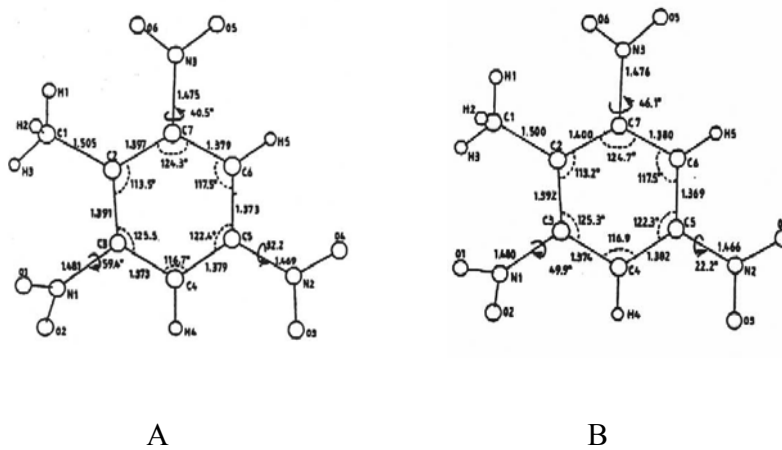
Figure 2.2 Molecular forms A and B of monoclinic TNT
(From Gallagher, et al., 1997).
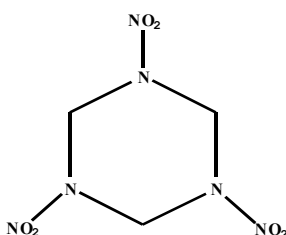
Figure 2.3 Chemical structure of RDX

Table 2.1 Physical and chemical properties of TNT
(From USDHS, 1995)

| property | Information |
|---|---|
| Molecular weight | 227.13 |
| Specific gravity | 1.654 |
| Melting points | 80.1$^o$C |
| Boiling points | 240$^o$C |
| Solubility | 130mg/L |
| Partition coefficients | |
| Log $K_{ow}$ | 1.60; 2.2(measured)-2.7(estimated) |
| $K_{oc}$ | 300(estimated)-1100(measured) |
| Vapor pressure (20$^o$C) | 1.99x10$^{-4}$mmHg |
| Henry's constant | 4.57x10$^{-7}$atm.m$^3$/mole |
| Flashpoint | explodes |
| Explosive temperature | 464$^o$F |

# CHAPTER 3

# ALKALINE HYDROLYSIS

## 3.1 Introduction

Alkaline hydrolysis was identified in the previous chapter as a promising method for destruction of high explosives. Alkaline hydrolysis uses E2-elimnation as a destruction mechanism. E2-elimination is the most important elimination mechanism in organic chemistry and follows a second-order rate law. If the base also shows nucleophilic character, it is accompanied by a nucleophilic substitution at an electron-poor C-atom, which occurs in RDX's heterocyclic system when it is destroyed by alkaline hydrolysis. Hantzsch and Kissel (1899) discovered that TNT could be attacked by nucleophilic molecules. This reactivity with base is due to the electron withdrawing nature of the nitro groups (Jones *et al*., 1982).

Recently, several studies of alkaline hydrolysis of TNT and other nitroaromatics have been conducted and have focused on the identification of the intermediate species and by products. These treatment technologies may be limited to aqueous TNT systems (as opposed to bulk materials), but to provide valuable insights into the nature of the reactions

and by products.

The hydrolysis of TNT and other nitroaromatics results in the formation of highly colored solutions (Urbanski, 1964). In this study, it also states that when TNT reacts with alkalis, a considerable change occurs that yields red or brown colored by-products. Organic substances that are no longer energetic can be separated from these products. The by products were unknown, and no more recent references to identify it have been found.

The majority of experiments evaluating the reaction of TNT with various bases have occurred at or below room temperature. Buncel *et al*, (1968) observed methyl protons of TNT in basic medium (90% dimethylfomamide-10% $D_2O$) exchanged with the hydrogen ions. The solution rapidly discolored and attempts to recover unreacted TNT but were unsuccessful.

## 3.2 Intermediates

The formation of highly colored solutions when TNT reacts with strong bases has been attributed to the production of the intermediate 2,4,6-trinitrobenzyl anion ($TNT^-$) (Blake *et al*, 1966). In solvent systems of methanol, ethanol, or 50% dioxane-50% water, three fast kinetic processes have been identified (Bernasconi, 1971). In excess base, the

formation of TNT⁻ is the principal process; at relatively high base concentrations a faster

process occurs that has not yet been accurately characterized, but may be due to a

Meisenheimer complex coupled to a radical-anion formation. When TNT is in excess

relative to the base, the formation of a Janovsky complex, which is a coupling of TNT⁻ with

a second TNT molecule, is observed. The various species are illustrated in Figure 3.1. The

comparison of the spectrum of TNT in excess base in 10% dioxane-90% water resulted in

markedly different results. The species formed has not been identified but showed that a

small change in medium can have a significant effect on the chemistry. Preliminary

analysis showed that radicals were formed and that TNT⁻, if formed at all, is very transient

(Bernasconi, 1971).

TNT also undergoes photolytic reactions in alkaline conditions. Hammersley (1975)

found that the replacement of a nitro group by a hydroxyl group is accelerated by exposure

to light in basic media. This observation has led to attempts to design treatment methods

that use UV radiation to remove TNT from solution.

Surfactants may enhance the rate of color formation involving reactions of TNT and

bases in aqueous solutions (Okamoto and Wang, 1975). It was assumed that the coloration

resulted from TNT⁻ and the increased rate was due to minor effects.

The anion and complexes, showed in Figure 3.1, are themselves relatively reactive intermediates that can produce other species depending upon the medium and conditions under which the reactions occur.

**3.3 End Products**

Only little progress has been made in their identification due to the many potential products arising from TNT hydrolysis. Some of the species already identified are anilines, dinitrobenzenes, nitroanalines as well as toluene, ethylbenzene and various long chain saturated hydrocarbons such as hexadecane and tetradecane (Riemer, 1995).

The identification of possible products and reaction mechanisms is complicated by the nature of the hydrolysis reaction. The chemistry makes possible the production of all reduced forms of $CH_3$ and $NO_2$, which can result in anthranils, alcohols, and aldehydes, as well as nitroso, nitril, azo and azoxy compounds among others (Riemer, 1995).

The efficiency of alkaline hydrolysis as a treatment method will depend on the identification of the major hydrolysis products. Hydrolysis has been proven to transform TNT into non-energetic compounds (Saupe *et al*., 1996 and Spontarelli *et al*., 1993). Heilmann *et. al*., (1996) showed that alkaline hydrolysis can effectively regenerate

activated carbon that is loaded with the high explosives RDX and HMX. Based on these

earlier results, the use of this technology for treatment of TNT contaminated wastes

appears promising.

**3.4 Reaction constants for TNT alkaline hydrolysis**

**3.4.1 Chemical Kinetics**

From previous studies (Heilmann and Stenstrom, 1996) of alkaline hydrolysis of

HMX and RDX, it was suggested the alkaline hydrolysis of these two explosives follows

the E2-mechanism. Hence, a second-order rate equation is also used to model the chemical

reaction for alkaline hydrolysis of TNT. The equation of second-order rate expression is

shown below.

$$\frac{dC_{TNT}}{dt} = -k_2 C_{TNT} C_{OH} \qquad (3.4.1)$$

Where $k_2$ is the second-order rate constant and $C_{TNT}$ and $C_{OH}$ represent the TNT and

hydroxide concentration, respectively. In the presence of excess base, we can assume

hydroxide concentration is constant, a pseudo first-order rate equation can be used:

$$\frac{dC_{TNT}}{dt} = -k_1 C_{TNT} \qquad (3.4.2)$$

Where $k_1 = k_2 C_{OH}$

By integrating the equation with initial concentration $C_{TNT}{}^0$, final concentration $C_{TNT}$

with respect to time, one obtains:

$$ln\,\frac{C_{TNT}}{C_{TNT}^0} = -k_1 t \qquad\qquad (3.4.3)$$

By plotting the *log* $C_{TNT}$ versus time, the pseudo first-order rate constant can be

obtained trough a linear regression of the experimental data.

Priesley (1998) performed a series of experiments at various OH$^-$ concentrations and

temperatures to determine the pseudo first-order rate constant The second-order rate

constant can be calculated from the first-order rate constant at constant temperature and

varying OH$^-$ concentrations from the equation $k_2 = k_1 / C_{OH}$.

**3.4.2 Kinetic Experiments**

Three different pHs (11.5, 12.0, and 12.5) were used (OH$^-$ concentrations of 6.5

mM/L, 21 mM/L, and 68.5 mM/L, respectively). The experiments were performed at

temperatures of 20°C, 50°C, and 80°C.  Significant transformation of TNT occurred under

all conditions studied.  Figure 3.2 displays the kinetic results from the alkaline hydrolysis

of TNT at a hydroxide concentration of 6.5 mM/L (pH = 11.5) carried out at various

temperatures (Priestley, 1997).  Transformation rates increased with increasing hydroxide

concentration with over two-thirds of the initial TNT concentration being transformed after

60 minutes at 20°C and 91% after 10 minutes at 80°C. No TNT was detected after 12.5

minutes at 80°C. Figures 3.3 and 3.4 show the kinetic results of the alkaline hydrolysis

over the same temperature range for hydroxide concentrations of 21 mM/L (pH 12.0) and

68.5 mM/L (pH 12.5), respectively. The remaining concentration of TNT was

undetectable after 6 minutes at pH 12.5 and 80°C.

In order to apply the pseudo first-order rate model, the hydroxide concentration must

remain relatively constant throughout the experiment. To validate the assumption, two

measurements were suggested (Priestley, 1998): Measured $OH^-$ concentration at the end of

the experiment should not change significantly from the starting concentration, or the log

concentration versus time relationship should be linear.

Hydroxide concentrations were measured at both the beginning and end of each

experiment and did not vary more than ± 3%. The highest degree of linear correlation was

found at 80°C ($R^2$ values ranging from 0.95 - 0.96). The lowest degree of correlation

occurred at pH 12.0, 50°C; pH 12.5, 50°C; and pH 11.5, 20°C ($R^2$ values of 0.80, 0.84, and

0.89, respectively). All other correlation coefficients were above 0.94. Therefore, the

pseudo first-order model is deemed applicable over the pH (11.5-12.5) and temperature

(20°C to 80°C) conditions of the experiment.

The pseudo first-order rate constants ($k_1$) and the related $R^2$ correlation coefficients are presented in Table 3.1.  Since the calculation of the second-order rate constants from the pseudo first-order rate data magnifies the impact of any error, the pH 12.0 and pH 12.5 at 50°C, and pH 11.5 at 20°C measurements were not used.  Approximate second-order rate constants are 0.0926 L/mol·min, 0.222 L/mol·min, and 6.67 L/mol·min at 20°C, 50°C and 80°C, respectively.

The rate of aqueous homogeneous alkaline hydrolysis of TNT in the presence of OH⁻ increases with both temperature and OH⁻concentration.  However, it appears that an increase in OH⁻ concentration at temperatures above 50°C has an inhibitory effect on the rate.  Due to the poor linear correlation at 50°C, this relationship is uncertain, and requires further investigation.

Table 3.1 Pseudo first-order rate constants and correlation coefficients
for the aqueous alkaline hydrolysis of TNT (From Priestley, 1998)

| $k_1$ (min$^{-1}$) | | | |
|---|---|---|---|
| Temperature (°C) | 6.5 mmol OH-/L (pH 11.5) | 21 mmol OH-/L (pH 12.0) | 68.5 mmol OH-/L (pH 12.5) |
| 20 | 0.00835 | 0.00719 | 0.0116 |
| 50 | 0.0212 | 0.0410 | 0.350 |
| 80 | 0.0951 | 0.529 | 0.510 |
| $R^2$ (correlation coefficient) | | | |
| 20 | 0.8871 | 0.9432 | 0.9878 |
| 50 | 0.9795 | 0.7988 | 0.8363 |
| 80 | 0.9611 | 0.9484 | 0.9745 |

Trinitrobenzyl Anion          Meisenheimer  Complex

Janovsky Complex
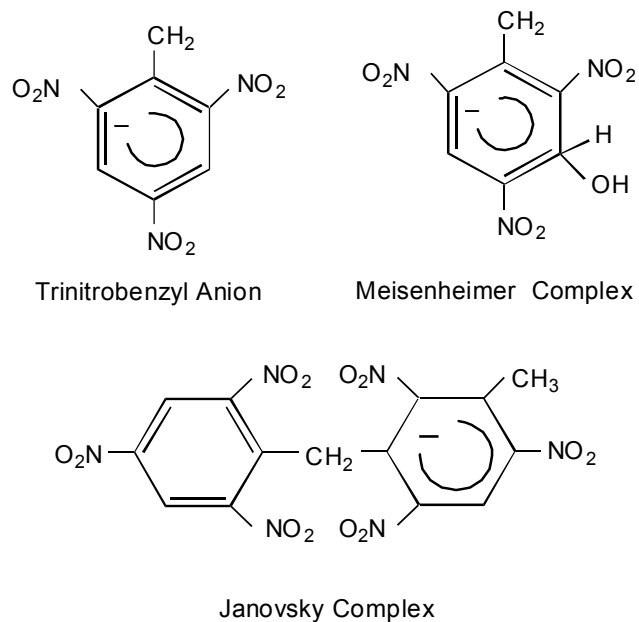
Figure 3.1 Chemical Structure of TNT Intermediates
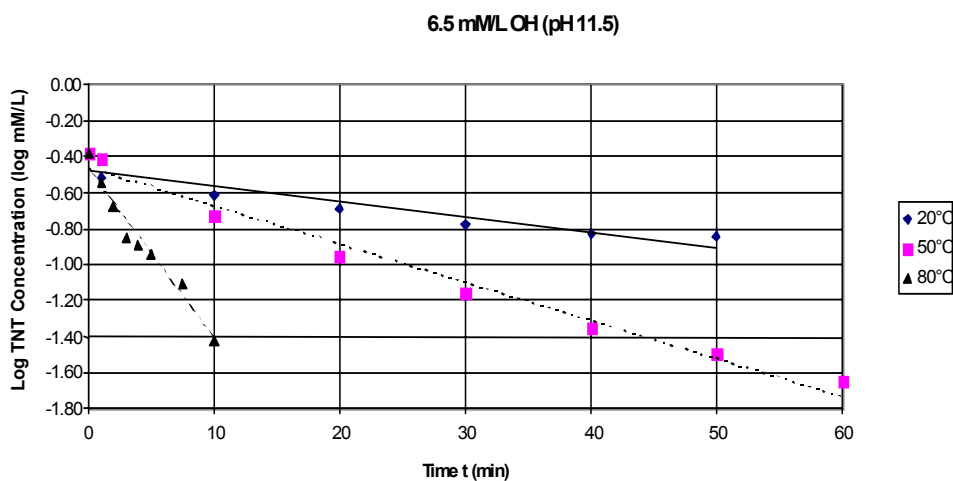


Figure 3.2 *Log $C_{TNT}$* versus time, pH=11.5; OH$^-$ concentration
6.5mM/L. (From Priestley, 1998).

**21 mM/L OH⁻ (pH 12.0)**
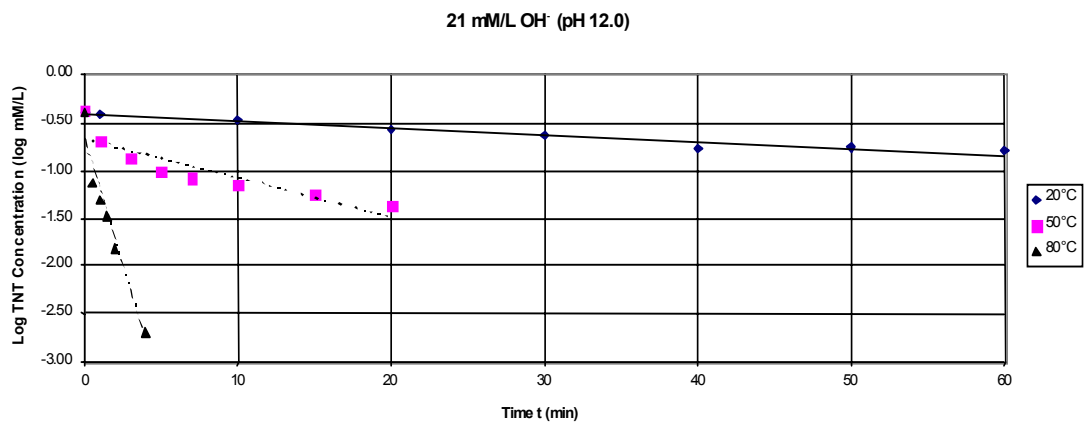


Figure 3.3 *Log C$_{TNT}$* versus time, pH=12.0; OH⁻ concentration 21mM/L.
(From Priestley, 1998).

**68.5 mM/L OH⁻ (pH 12.5)**
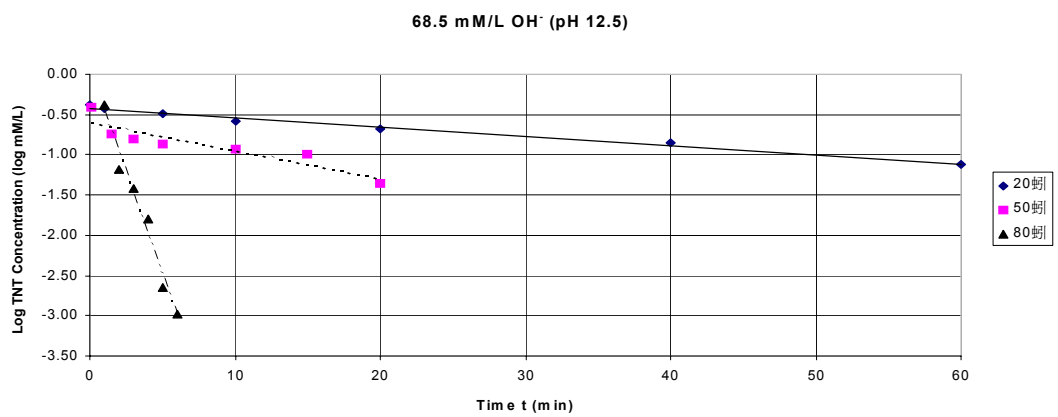


Figure 3.4 *Log C$_{TNT}$* versus time,  pH=12.5; OH⁻ concentration 68.5mM/L.
(From Priestley, 1998).

# CHAPTER 4

# DIFFUSION COEFFICIENTS OF TRINITROTULENE

## 4.1 Introduction

Diffusion coefficients are an important factor required when modeling TNT alkaline hydrolysis treatment. The total mass transfer rate-limiting step is often controlled by diffusion. Therefore, to determine the rate of diffusion, it is necessary to measure diffusion coefficient.

## 4.2 Methods to Measure Diffusion Coefficients

There are several recognized methods to measure diffusion coefficients, which have are easy and accurate. Among them, the diaphragm, infinite couple and Taylor dispersion methods are considered simple yet efficient. For measuring the TNT diffusion coefficient, we used the diaphragm cell, which will be described later in this chapter. The infinite couple and Taylor dispersion are described in this section.

The infinite couple is often applied in measuring diffusion coefficients of solids. It consists of two solid bars differing in composition. To start an experiment, the two bars are joined together and quickly raised to the temperature at which the experiment is to be made. After a known time, the bars are quenched and the composition is measured as a function of position. The concentration profile is

$$\frac{c_1 - \bar{c}_1}{c_{1\infty} - \bar{c}_1} = erf\left(\frac{z}{\sqrt{4Dt}}\right) \tag{4.2.1}$$

where $c_{1\infty}$ is the concentration at that end of the bar where $z = \infty$ and $\bar{c}_1$ is the average concentration in the bars. The measured concentration profile is fit numerically to determine the diffusion coefficient.

The Taylor dispersion method uses a long tube filled with solvent that slowly moves in laminar flow. A sharp pulse of solute is injected near one end of the tube. When this pulse comes out the other end, its shape is measured with a differential refractometer. The concentration profile found in this apparatus is the same as the decay of a pulse

$$c_1 = \frac{M}{\pi R_0^2} \frac{e^{-z^2/4Et}}{\sqrt{4\pi Et}} \tag{4.2.2}$$

where $M$ is the total solute injected, $R_0$ is the tube radius. $v^0$ is the average velocity of the flowing solvent, and E is a dispersion coefficient given by

$$E = \frac{\left(v^0 R_0\right)^2}{48D} \tag{4.2.3}$$

Because the refractive index varies linearly with the concentration, the refractive-index profile can be used to find the concentration profile and the diffusion coefficient.

## 4.2.1 Diaphragm Cell

The Stokes diaphragm cell is probably the best tool to measure diffusion coefficients because it is inexpensive and simple, and the error is as low as 0.2% (Cussler, 1997).

The diaphragm cell consists of two compartments separated by a glass frit or by a porous membrane (Stokes, 1950). The solutions in compartments are kept well mixed by a rotating magnet. Figure 4.1 shows the apparatus.
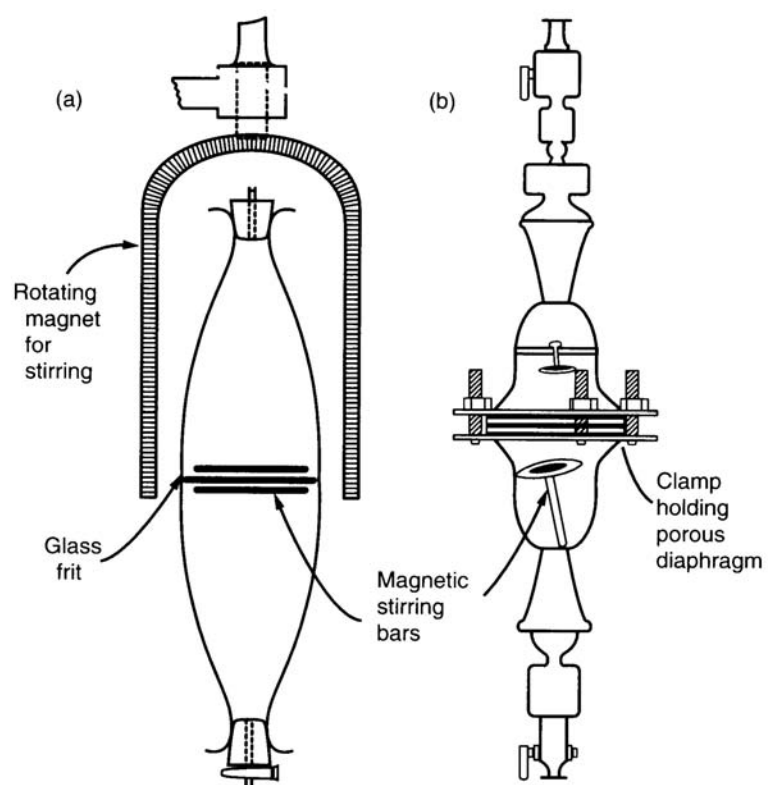
Figure 4.1 Diffusion cells (left using a glass frit, generally considered more accurate than the left cell that uses filter paper, (From Cussler, 1997).

It is usually assumed that the diffusion process is pseudo-steady state. The flux passing through the diaphragm is

$$J = \frac{DH}{l}(C_{i,donor} - C_{i,receptor})$$ (4.2.4)

where $J$= flux through diaphragm, $l$= effective thickness of diaphragm.

$H$= available diffusion coefficient fraction of the diaphragm area.

$C_{i,donor}$= concentration of donor compartment and $C_{i,receptorr}$= concentration of receptor compartment.

$$V_{donor} \frac{dC_{i,donor}}{dt} = -AJ$$ (4.2.5)

$$V_{receptor} \frac{dC_{i,receptor}}{dt} = +AJ$$ (4.2.6)

where $A$= area of diaphragm, $V_{donor}$ = volume of the donor compartment. And $V_{receptor}$= volume of the receptor compartment.

$$\frac{d}{dt}(C_{i,donor} - C_{i,receptor}) = D\beta(C_{i,donot} - C_{i,receptor})$$ (4.2.7)

The cell constant $\beta$ is defined as follows:

$$\beta = \frac{AH}{l}\left(\frac{1}{V_{donor}} + \frac{1}{V_{receptor}}\right)$$ (4.2.8)

and the initial condition is

$$C_{i,donor} - C_{i,receptor} = C_{i,donor}^{o} - C_{i,receptor}^{o}$$ (4.2.9)

After integrating and substituting the initial condition we can get

$$D_i = \frac{1}{\beta t} \ln\left[\frac{(C^o_{i,donor} - C^o_{i,receptor})}{(C_{i,donor} - C_{i,receptor})}\right]$$ (4.2.10)

The cell constant β should be determined by calibration using a solute whose diffusion coefficient is known. A KCl –water solution is often used.

If the ratio of relaxation time of the diaphragm ($l^2/D$) to diffusion room relaxation time ($1/D\beta$) is much smaller than one, the pseudo-steady state approximation is suitable. The conditions are shown in equation 4.2.11.

$$1 >> \frac{l^2/D}{1/\beta D} = V_{diaphragm}\left(\frac{1}{V_{donor}} + \frac{1}{V_{receptor}}\right)$$ (4.2.11)

The experimental results can be substituted into the equation to examine assumption of pseudo-steady approximation.

The TNT concentrations of the donor and receptor cells were measured with an HPLC procedure using a C18 column, and is described later. The diffusion coefficient will vary with temperature, and should be determined at 3 or 4 different temperatures: $20^oC$ and other temperatures (depends on the reaction coefficients of known temperature).

## 4.3 Experiment Procedure

### 4.3.1. Diaphragm Design

It is necessary to design and construct a diaphragm cell since there are no commercial manufacturers. Previous studies applying membranes as diaphragms have been successful in measurement of insulin and TRH (Chou, 1996). Hence, the membrane design diaphragm was selected. To maintain uniform concentration in each compartment without gradients, stirring is necessary which was provided by round stirring bars

(Nalgene Star Head magnetic stir bars) in the bottom of each compartment. Temperature is controlled and maintained by water jackets around each compartment. Thermometers (Fisher Scientific) were used in the process of the experiment to monitor the temperature. Figure 4.2 illustrates our design.

**4.3.2 HPLC standardization**

High grade TNT was obtained from Lawrence Livermore National Laboratory. HPLC grade water was used in the solution preparation. Phenol or toluene-water system was used to calibrate the cell constant, $\beta$. Toluene and phenol were selected because they are similar to TNT  (aromatic) and they can be detected by the same HPLC/C18 column procedure.

Samples were measured using an HPLC (Hewlett Packard 5270) with a variable wavelength detector and autosampler. Separation were made using a 25 cm, adsorbosphere, C18, reverse-phase column (4.6 mm I.D.) and corresponding 5 mm guard column.  Standard curves were developed for each compound and measurements were kept within the linear range of the HPLC by appropriate dilutions.

Phenol stock solution (1mg/ml) was used to prepare standard solutions with different concentrations. Phenol was detected at 254nm. The mobile phase was composed of 58% acetonitrile and 42% water at flow rate of 1.0 ml/min. The retention time for phenol was approximately 3.7 min. Figure 4.3 shows the phenol standardization.

Toluene standards solution was prepared in a similar way. However, due to the low solubility of toluene, a 50% methanol-water solution was used to facilitate dissolution. The flow rate was 1.5 ml/min and the wavelength was 254 nm. The mobile phase was

composed of 60% acetonitrile and 40% water. The retention time was approximately 4.2 min.

Figure 4.4 shows the first standardization of toluene. The standardization shows variability especially at 600 mg/L. Various reasons may be responsible, including stratification (toluene is lighter than water) and volatilization. A second procedure using greater mixing and elimination of head space produced more precise results as shown in. Figure 4.5.

For TNT analysis, Priestley (1997) used a mobile phase of 50% water and 50% methanol at a flow rate of 1.5 ml/min which produced a retention time of 6.4 minutes. A slightly different condition was developed for this study, which used a mobile phase composed of 50% acetonitrile, 10% water and 40% methanol at flow rate of 1.5 ml/min. The retention time was approximately 4.25 min. The detection wavelength for both procedures was 236nm. Figure 4.6 shows the standard curve.
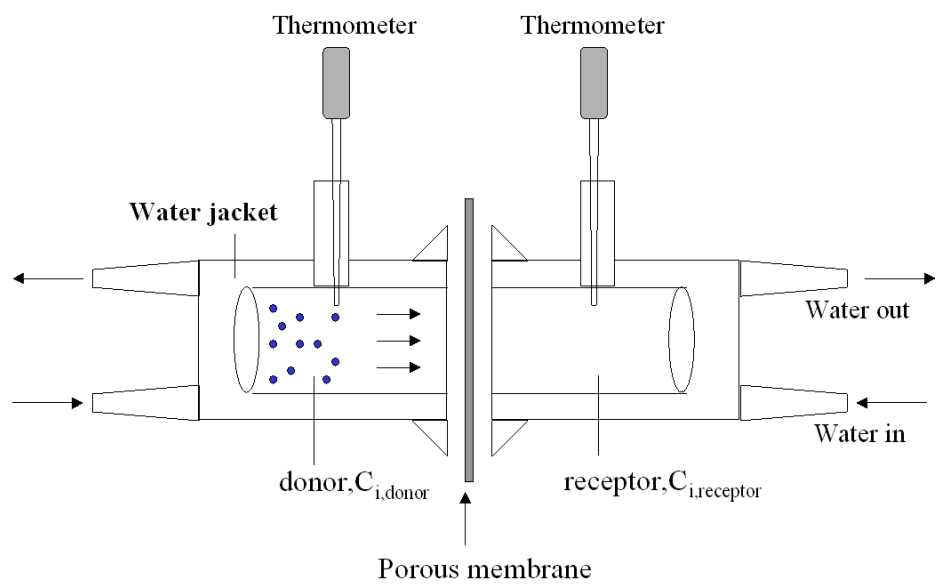
Figure 4.2 Diaphragm cell design
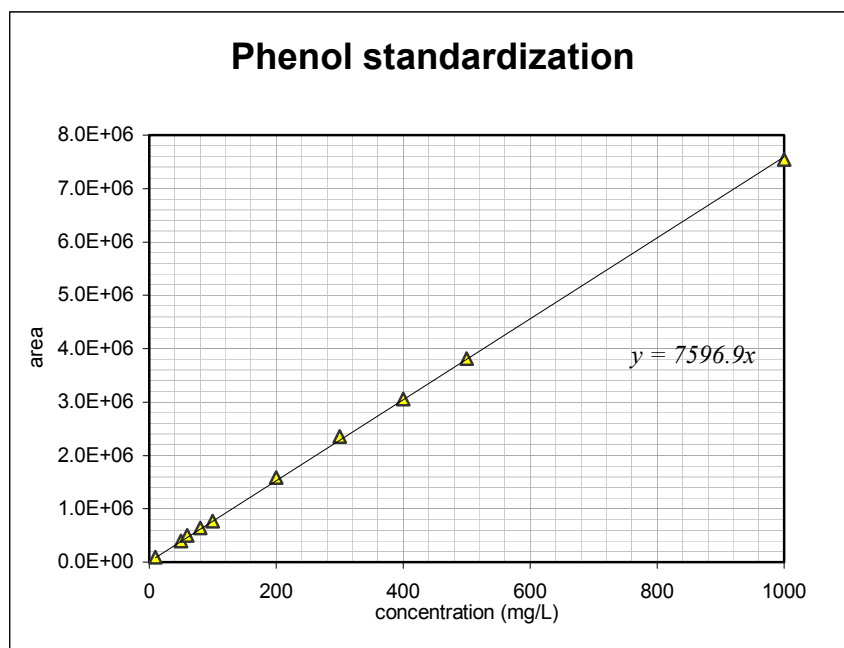
Figure 4.3 Standardization of phenol, flow rate 1.0ml/min, λ=254nm.
Mobile phase : 52 acetonitrile, 48% water.

**Toluene Standardization(1)**

$y = 565.21x$

Area

Concentration (mg/L)
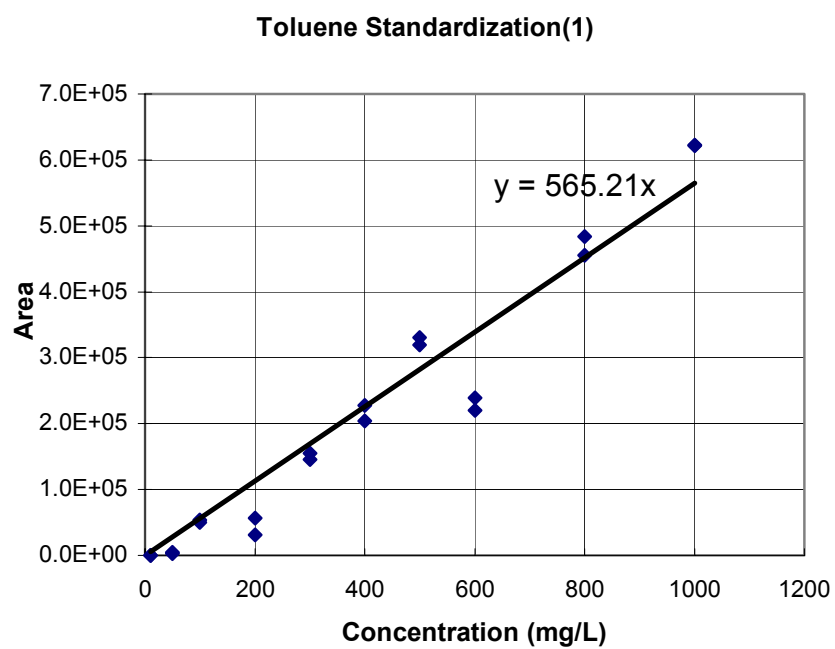
Figure 4.4 First standardization of toluene, flow rate 1.5ml/min,
λ=254nm. Mobile phase : 60% acetonitrile, 40% water

## Toluene Standardization
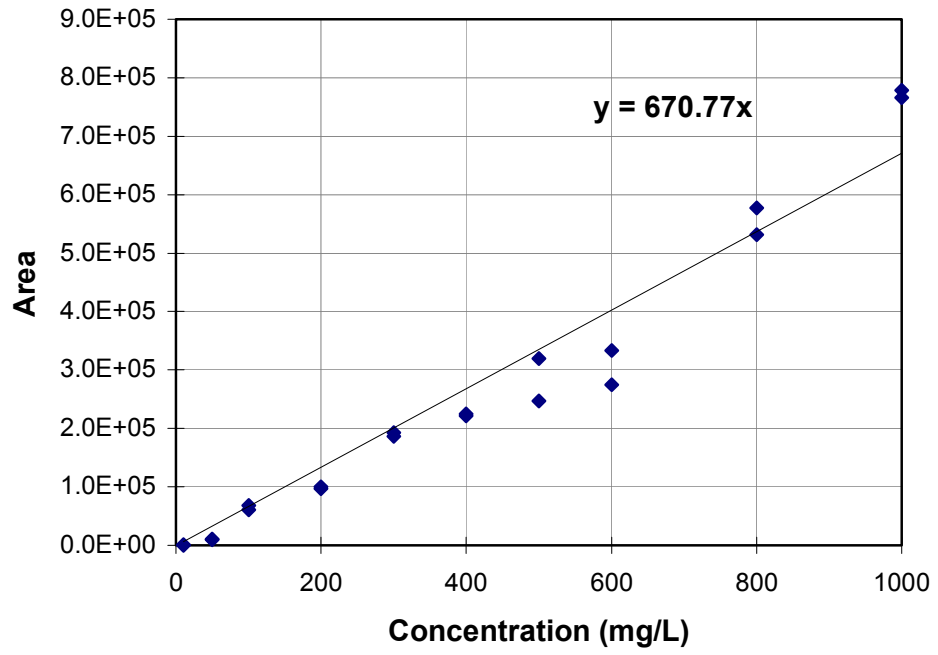


Figure 4.5 Second standardization of toluene, flow rate 1.5ml/min, λ=254nm. Mobile phase: 60% acetonitrile, 40% water

**TNT Standardization**
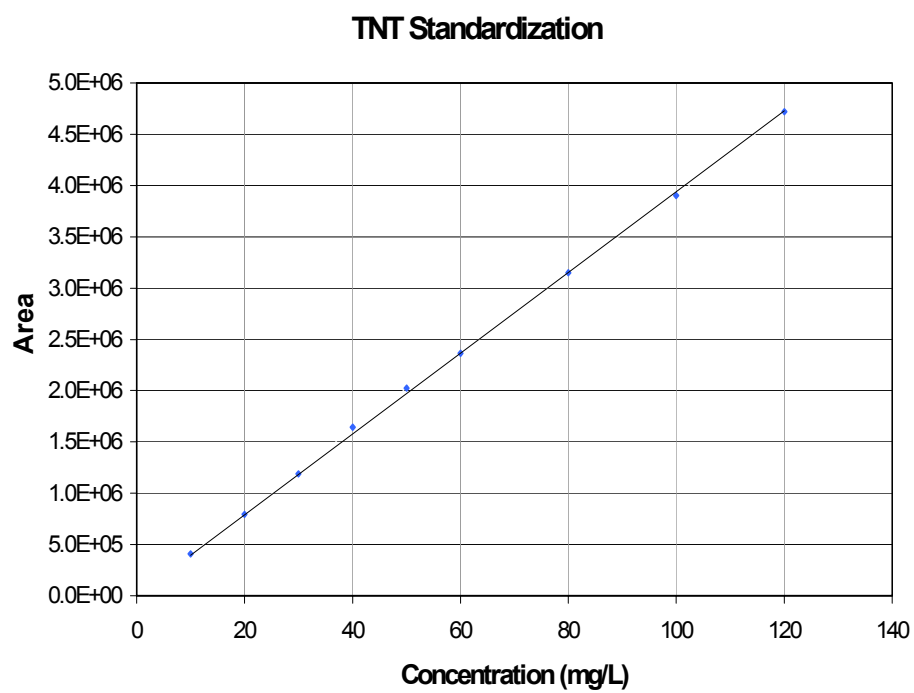
Figure 4.6 Standardization of TNT, flow rate 1.5ml/min, ,
λ=236nm. Mobile phase : 50% methanol, 10%
acetonitrile, 40% water.
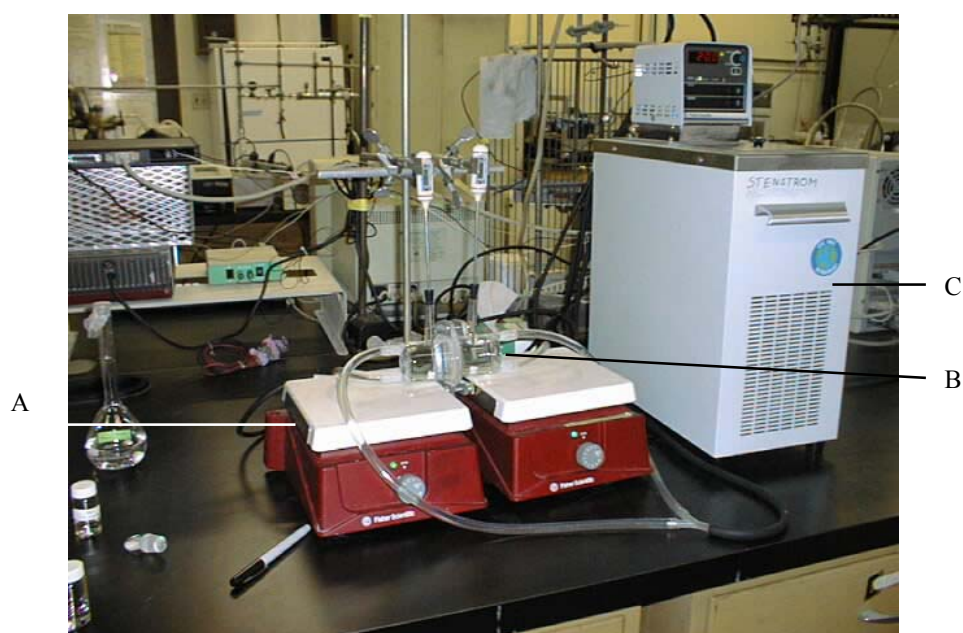
Figure 4.7 Experiment set-up.
    A.   Magnetic stirring plate.
    B.   Diaphragm cell.
    C.   Water bath.

### 4.3.3 Experiment Set-up and Procedure

Figure 4.7 shows the experimental set-up.  The diaphragm cell was located between two magnetic stirring plates. A cellulose acetate membrane (diameter 4.7cm, pore size 0.45μm, 0.02cm thickness, Fisher Blend) was used to separate two compartments and provided channels for diffusion. The water jackets were connected with tubes to a water bath (model 8005, Fisher scientific), which heats or cools to maintain the constant temperature. Thermometers were used to monitor temperature.

A water bath was used to insure that both solutions and the cell were at constant temperature.  This was performed in a water bath set to the prescribed temperature (i.e., $20^{o}$C in the first case). The water bath contained an open area to receive flasks and a pump to circulate water through a manifold.  After the water bath reached constant temperature, two containers were placed in the bath. One container held HPLC grade water to be used for the receptor side and the other contained HPLC water plus the compound to be analyzed.  Water from the bath circulated through a manifold wrapped around the diffusion cells. After one hour, both solutions and the cells equilibrated to the set point temperature.  After equilibration both cells were injected with donor and receptor solutions (38 ml each), and the stirrers were started.  Samples were also taken from the stock solutions to represent initial concentrations.

After a period of time (about 3 hours in most experiments), samples were collected and analyzed with the HPLC for both initial and final solutions. The results were substituted into equations 4.2.10 to calculate the diffusion coefficient.

## 4.4 Results and Discussion

### 4.4.1 Cell Constant β Calibrated with Phenol

After 3 hours of mixing phenol was detected in the receptor compartment and a decrease was observed in the donor compartment also. Because the response is proportional to the concentration, it can be substitute into the constant equation as follows:

$$\beta = \frac{1}{D_{ph}t}\ln\left[\frac{(C_{ph,donor}^{o} - C_{ph,receptor}^{o})}{(C_{ph,donor} - C_{ph,receptor})}\right] \tag{4.3.1}$$

where $D_{ph}$ is diffusion coefficient of phenol in $20^{\circ}C$; $D_{ph} = 0.89 \times 10^{-5} cm^{2}/s$ .(CRC Handbook, 1997). The experiment was repeated several times, which yielded a mean constant β =4.05 $cm^{-2}$. The measured range was 3.6 to 4.7 $cm^{-2}$. Table 4.1 shows the results of the cell constants calculated using phenol.

### 4.4.2 Cell Constant β Calibrated by Toluene

The cell constant was measured again using toluene, which has a diffusivity of $D_{toluene} = 0.8669 \times 10^{-5} cm^{2}/s$ (CRC Handbook, 1997). Toluene is much more volatile that phenol and loss due to volatilization creates error in the cell constant calculation. Therefore the headspaces of each bottle and vial was decreased to reduce experimental errors. Stirring time was also minimized; however, large errors still occurred as shown in Table 4.2.  To understand the experimental error due to toluene volatilization, an experiment was conducted quantify its loss over time. The standard solution of toluene

45

was placed in a closed system, and measured after 1, 2, and 3 days. The results are shown in Figure 4.8. The loss was estimated using an exponential function. An error analysis was also performed, as follows:

$$Scd_o - Scr_o = \sqrt{S^2 cd_o} = Scd_o \qquad (4.3.1)$$

$$Scd - Scr = \sqrt{S^2 cd + S^2 cr} \qquad (4.3.2)$$

$$\beta = \frac{1}{Dt} \ln\left[ \frac{Scd_o - Scr_o}{Scd - Scr} \right] \qquad (4.3.3)$$

$$S_\Delta = S_{\Delta AVG} \cdot \sqrt{\left(\frac{S_{\Delta o}}{Scd}\right)^2 + \left(\frac{S_\Delta}{Scd}\right)^2} \qquad (4.3.4)$$

$$S_\beta = \frac{S_{\Delta AVG} \sqrt{\left(\frac{S_{\Delta o}}{Scd}\right)^2 + \left(\frac{S_\Delta}{Scd}\right)^2}}{\beta_{AVG}} \qquad (4.3.5)$$

The error analysist is shown in Table 4.3. The mean cell constant $\beta$ using toluene is $6.15 \pm 2.53 cm^{-2}$, which is much larger and more variable than the value measured for phenol ($4.05 \pm 0.56 cm^{-2}$).

### 4.4.3 Toluene Volatilization Interference on Cell Constant Determination

Cell constant $\beta$ should be independent from the compound used in its analysis. The greater constant measured using toluene as compared to phenol or KCl (see next section) suggests experimental error. To better understand the potential sources of error, Henry's Law was used to estimate the toluene loss due to volatilization. The experimental procedure as follows

1. Prepare 250 ml standard toluene solution at 500 mg/L concentration.

2. Determine the headspace of each side of the diaphragm cell, which was 3 ml. (the total volume of each side is 37 ml).

3. The stock standard solution was placed in each side of the diffusion cell and in sealed controls, which had no headspace.

The toluene loss was measured and calculated as a percentage of the total present. The toluene concentration in water will decrease and the concentration in air will increase. The Henry's coefficient for toluene is $K_H$=0.271 (dimensionless)

Cdo= 527 mg/L, Cro=0 mg/L; Cd=384 mg/L, Cr=81mg/L

Cdo: initial concentration of donor side; Cro: initial concentration of receptor side. Cd: final concentration of donor side; Cr: final concentration of receptor side.

The average toluene concentration in water, donor side, during experiment was 456 mg/L. The average toluene concentration in water, donor side, during experiment was 41 mg/L

$$K_H = \frac{Ca}{Cw} = 0.271 \qquad (4.3.6)$$

Mass balance in donor site was

$$VaCa + VwCw = VwC'w \qquad (4.3.7)$$

Substuting the values, $C'w$=476 mg/L ($C'w$ is the average of Cdo and Cd, and Cd is not affected by the evaporation) $C'd$=424 mg/L, and applying a mass balance to the receptor site, the correlated $C'r$ becomes 83 mg/L.

The correlated cell constant β becomes

$$\beta = \left(\frac{1}{Dt}\right)\ln\left(\frac{Cdo - Cro}{C'd - C'r}\right) = \left(\frac{1}{Dt}\right)\ln\left(\frac{527}{424 - 83}\right) = 4.76 \qquad (4.3.8)$$

The value of 4.76 is much closer to the value measured with phenol.


### 4.4.4 Cell Constant β Calibrated by KCl

Because the cell constant calculated from toluene had errors, a commonly used labeling compound, potassium chloride, was also used to measure the cell constant. 200 mg/L potassium chloride was prepared to run the experiment. It has been noted that the diffusion coefficient of KCl varies with its concentration (Cussler, 1997) and Table 4.4 shows its concentration. . The KCl concentration was determined by ion chromatography. The standardization was done in previous work (see chapter 4.2). Table 4.4 lists the results. The mean cell constant was 4.3, close to the value measured with phenol and the correlated one with toluene.  Based upon these results, an average cell constant of 4.1 was used in the TNT measurements.

### 4.4.5 TNT Diffusion Coefficient

To measure the TNT diffusivity, a 100mg/L TNT standard solution was prepared with 50mg TNT and adding HPLC grade water to 500ml.  The solution was allowed to reach thermal equilibrium before conducting the experiment and all other conditions were the same as in the calibration experiments.  According to the data, the TNT diffusion coefficient is $D_{TNT} = 1.18 \times 10^{-5} cm^2/s$. Table 4.5 is the result of experiment.

Table 4.1 Cell constant β calibrated by phenol

| Cdo(mg/L) | Cro(mg/L) | Cd(mg/L) | Cr(mg/L) | Beta |
|---|---|---|---|---|
| 397.52 | 0.00 | 363.40 | 62.61 | |
| 398.23 | 0.00 | 363.59 | 48.56 | 2.67 |
| 397.52 | 0.00 | 333.34 | 78.08 | |
| 398.23 | 0.00 | 331.99 | 67.61 | 4.43 |
| 397.52 | 0.00 | 340.91 | 62.49 | |
| 398.23 | 0.00 | 345.18 | 62.91 | 3.64 |
| 415.99 | 0.00 | 344.39 | 63.86 | |
| 415.73 | 0.00 | 347.28 | 58.91 | 3.95 |
| 407.52 | 0.00 | 342.48 | 73.65 | |
| 407.33 | 0.00 | 342.49 | 73.74 | 4.33 |
| 410.16 | 0.00 | 348.27 | 65.15 | |
| 410.86 | 0.00 | 339.94 | 69.40 | 4.10 |
| 412.60 | 0.00 | 349.19 | 85.27 | |
| 413.84 | 0.00 | 344.74 | 83.12 | 4.71 |
| 407.53 | 0.00 | 340.57 | 82.09 | |
| 429.69 | 0.00 | 337.37 | 56.66 | 4.58 |
| **Average** | | | | **4.05** |

Cdo is initial concentration of donor cell;  Cro is the initial
concentration of receptor cell; Cd is the final concentration of the
donor cell; Cr is the final concentration of the receptor cell. All are in
HPLC area units.

Table 4.2 Cell constant β calibrated by toluene

| Cdo(mg/L) | Cro(mg/L) | Cd(mg/L) | Cr(mg/L) | beta |
|---|---|---|---|---|
| 639.76 | 0.00 | 438.52 | 89.74 | 6.61 |
| 615.97 | 0.00 | 458.61 | 68.94 | 4.99 |
| 545.67 | 0.00 | 326.76 | 82.69 | 8.76 |
| 550.00 | 0.00 | 352.56 | 38.53 | 6.10 |
| 592.38 | 0.00 | 435.67 | 106.35 | 6.40 |
| 615.90 | 0.00 | 407.90 | 86.32 | 7.08 |
| 593.10 | 0.00 | 529.18 | 109.33 | 3.76 |
| 678.86 | 0.00 | 521.44 | 132.85 | 6.08 |
| 595.04 | 0.00 | 361.31 | 92.85 | 8.67 |
| 648.84 | 0.00 | 369.17 | 106.35 | 9.84 |
| 473.28 | 0.00 | 370.23 | 70.08 | 4.96 |
| 476.99 | 0.00 | 473.28 | 66.38 | 1.73 |
| 611.46 | 0.00 | 470.75 | 117.66 | 5.98 |
| 630.20 | 0.00 | 500.66 | 107.72 | 5.15 |
| **Average** | | | | 6.15 |

Cdo is initial concentration of donor cell;  Cro is the initial
concentration of receptor cell; Cd is the final concentration of the
donor cell; Cr is the final concentration of the receptor cell.

Table 4.3 Error analysis of statistical method

| Cell constant b calibrated by toluene | | | | | |
|---|---|---|---|---|---|
| time | Cdo | Cro | Cd | Cr | beta |
| 10800 | 639.76 | 0.00 | 438.52 | 89.74 | 6.61 |
| 10800 | 615.97 | 0.00 | 458.61 | 68.94 | 4.99 |
| 10800 | 545.67 | 0.00 | 326.76 | 82.69 | 8.76 |
| 10800 | 550.00 | 0.00 | 352.56 | 38.53 | 6.10 |
| 10800 | 592.38 | 0.00 | 435.67 | 106.35 | 6.40 |
| 10800 | 615.90 | 0.00 | 407.90 | 86.32 | 7.08 |
| 10800 | 593.10 | 0.00 | 529.18 | 109.33 | 3.76 |
| 10800 | 678.86 | 0.00 | 521.44 | 132.85 | 6.08 |
| 10800 | 595.04 | 0.00 | 361.31 | 92.85 | 8.67 |
| 10800 | 648.84 | 0.00 | 369.17 | 106.35 | 9.84 |
| 10800 | 473.28 | 0.00 | 370.23 | 70.08 | 4.96 |
| 10800 | 476.99 | 0.00 | 473.28 | 66.38 | 1.73 |
| 10800 | 611.46 | 0.00 | 470.75 | 117.66 | 5.98 |
| 10800 | 630.20 | 0.00 | 500.66 | 107.72 | 5.15 |
| **Average** | 590.53 | 0.00 | 429.72 | 91.13 | 6.15 |
| **Std Dev** | 60.29 | 0.00 | 66.09 | 24.70 | 2.53 |

Table 4.3 Error analysis of statistical method (continued)

| Cell constant b calibrated by phenol | | | | | |
|---|---|---|---|---|---|
| time | Cdo | Cro | Cd | Cr | beta |
| 10800 | 397.52 | 0.00 | 363.40 | 62.61 | 2.90 |
| 10800 | 398.23 | 0.00 | 363.59 | 48.56 | 2.44 |
| 10800 | 397.52 | 0.00 | 333.34 | 78.08 | 4.61 |
| 10800 | 398.23 | 0.00 | 331.99 | 67.61 | 4.26 |
| 10800 | 397.52 | 0.00 | 340.91 | 62.49 | 3.70 |
| 10800 | 398.23 | 0.00 | 345.18 | 62.91 | 3.58 |
| 10800 | 415.99 | 0.00 | 344.39 | 63.86 | 4.10 |
| 10800 | 415.73 | 0.00 | 347.28 | 58.91 | 3.81 |
| 10800 | 407.52 | 0.00 | 342.48 | 73.65 | 4.33 |
| 10800 | 407.33 | 0.00 | 342.49 | 73.74 | 4.33 |
| 10800 | 410.16 | 0.00 | 348.27 | 65.15 | 3.86 |
| 10800 | 410.86 | 0.00 | 339.94 | 69.40 | 4.35 |
| 10800 | 412.60 | 0.00 | 349.19 | 85.27 | 4.65 |
| 10800 | 413.84 | 0.00 | 344.74 | 83.12 | 4.77 |
| 10800 | 407.53 | 0.00 | 340.57 | 82.09 | 4.74 |
| 10800 | 429.69 | 0.00 | 337.37 | 56.66 | 4.43 |
| Average | 407.41 | 0.00 | 344.70 | 68.38 | 4.05 |
| Std Dev | 9.21 | 0.00 | 8.77 | 10.30 | 0.56 |

Table 4.4 Cell constant β calibrated by potassium chloride

**Cell constant b calibrated by Potassium Chloride**

| Cdo(mg/L) | Cro(mg/L) | Cd(mg/L) | Cr(mg/L) | Diffusion coeff | beta |
|---|---|---|---|---|---|
| 172.62 | 0.00 | 129.90 | 42.35 | $1.85 \times 10^{-5}$ | 3.41 |
| 172.00 | 0.00 | 135.39 | 42.59 | $1.85 \times 10^{-5}$ | 3.10 |
| 172.01 | 0.00 | 119.73 | 45.67 | $1.85 \times 10^{-5}$ | 4.23 |
| 184.10 | 0.00 | 153.50 | 54.50 | $1.99 \times 10^{-5}$ | 2.89 |
| 178.00 | 0.00 | 109.60 | 55.80 | $1.99 \times 10^{-5}$ | 5.58 |
| 221.90 | 0.00 | 103.10 | 55.50 | $1.98 \times 10^{-5}$ | 7.21 |
| 220.67 | 0.00 | 120.82 | 56.39 | $1.98 \times 10^{-5}$ | 5.77 |
| 206.63 | 0.22 | 151.14 | 33.69 | $1.98 \times 10^{-5}$ | 2.64 |
| 187.59 | 0.17 | 158.45 | 54.86 | $1.98 \times 10^{-5}$ | 2.77 |
| 226.71 | 0.00 | 118.45 | 42.88 | $1.97 \times 10^{-5}$ | 5.15 |
| 213.24 | 0.00 | 99.91 | 38.21 | $1.98 \times 10^{-5}$ | 5.81 |
| 176.87 | 0.05 | 146.73 | 37.01 | $1.99 \times 10^{-5}$ | 2.22 |
| 190.09 | 0.03 | 157.39 | 67.46 | $1.98 \times 10^{-5}$ | 3.49 |
| **Average** | | | | | 4.35 |

Cdo is initial concentration of donor cell;  Cro is the initial concentration of receptor cell; Cd is the final concentration of the donor cell; Cr is the final concentration of the receptor cell.

Table 4.5 TNT diffusion coefficient

| Cdo(mg/L) | Cro(mg/L) | Cd(mg/L) | Cr(mg/L) | D(cm$^2$/s) |
|-----------|-----------|----------|----------|-------------|
| 110.26 | 0.00 | 93.17 | 10.30 | |
| 110.01 | 0.00 | 92.67 | 10.33 | $0.63 \times 10^{-5}$ |
| 91.63 | 0.00 | 61.91 | 12.31 | |
| 86.99 | 0.00 | 61.99 | 17.68 | $1.42 \times 10^{-5}$ |
| 85.21 | 0.00 | 50.15 | 11.57 | |
| 87.38 | 0.00 | 52.20 | 10.63 | $1.69 \times 10^{-5}$ |
| 89.21 | 0.00 | 57.01 | 6.39 | |
| 88.25 | 0.00 | 59.10 | 6.35 | $1.19 \times 10^{-5}$ |
| 96.65 | 0.00 | 60.15 | 12.29 | |
| 96.95 | 0.00 | 60.35 | 12.35 | $1.55 \times 10^{-5}$ |
| 102.17 | 0.00 | 74.36 | 14.10 | |
| 102.95 | 0.00 | 71.57 | 13.05 | $1.20 \times 10^{-5}$ |
| Average | | | | $1.18 \times 10^{-5}$ |

Cdo is initial concentration of donor cell;  Cro is the initial concentration of receptor cell; Cd is the final concentration of the donor cell; Cr is the final concentration of the receptor cell.

## 4.5 Theoretical Estimation

In order to better understand the TNT diffusion coefficient, the experimental results were compared to well known theoretical methods of estimating diffusion coefficients. Methods proposed by Stokes-Einstein (Stokes, 1850; Einstein, 1905), Sutherland (1905), Glasstone et al. (1941), Scheibel (1954) and Wilke and Chang (1955). (Cussler, 1997).

The most common method to estimate diffusion coefficients from molecular properties is the Stokes-Einstein equation (Schwarzenbach, 1993). Cussler (1997) notes the method has limited accuracy with 20% or more error. The Stokes-Einstein equation is

$$D = \frac{k_B T}{6\pi\mu R_o} \qquad (4.3.9)$$

where $k_B$ is Boltzmann's constant, $\mu$ is the solvent absolute viscosity. And $R_o$ is the solute molecular radius. It should be noted that if the solute size is less than 5 times of the solvent radius, the Stokes-Einstein equation is not applicable.

Table 4.6 shows the governing equations for the other methods, which require a larger number of parameters. The Southerland and Glasstone et al. methods are very similar to equation 6.3.2 and require no additional parameters. The Scheibel and Wilke-Chang methods require additional parameters, which are discussed now. Both require the molar volumes, $\overline{V}$, at the boiling point. The Scheibel method uses an empirical constant, A, which was assumed to be $8.2 \times 10^{-8}$. The Wilke-Chang method requires a

$\phi$ factor which is equal to 2.26 for water. The method also uses molecular weight, $\overset{o}{M}$ and

the molar volume, $\widetilde{V}$, as a function of temperature. For TNT crystals, the molecular

weight is 227.13, and the specific gravity is 1.654, so the molar volume is 137.32 cm$^3$.

For the solvent (water), the molecular weight is 18, and the molar volume is 18 cm$^3$. The

viscosity of water will change with temperature. At T=20$^o$C the viscosity is 1 cp (10$^-$

$^2$g/cm·sec), and decreases to 0.5494 cp at T=50$^o$C and 0.3565 cp at T=80$^o$C. The radius

of TNT molecule is about 3.4 Å (Gallagher et al, 1997), which is an average of the two

molecular forms, A and B. The TNT we used is the yellow, odorless solid form, with the

monoclinic structure using AABBAABB packing motif. Therefore the molecular forms

A and B forms are in equal amounts. Table 4.7 shows the results of the four methods.

The predictions in Table 4.7 vary among methods but same order of magnitude.

The Stokes-Einstein and Sutherland methods are similar to the experimental results (0.63

and 0.95 x 10$^{-5}$ versus 1.1 x 10$^{-5}$ for the experimental results). The differences are

probably due to inaccurate parameters. The molar volume of TNT at boiling point is

impossible to measure because TNT explodes at 220$^o$C, which is lower than the boiling

point. The molar volume of solid TNT, 137.32 cm$^3$, to be used instead. The effect seems

not relevant in the predictions of the Scheibel and Wilke-Chang methods, which require

this parameter, since the expansion coefficient for TNT as the function of temperature is

not large. Temperature has a large impact for all methods, which is due to the viscosity

changing with temperature. Therefore, controlling temperature in the process of

measuring diffusion is critical to preserve accuracy.

Table 4.6 Theoretical and empirical equations used to estimate
diffusion coefficients (from Cussler, 1997).

| Author | Basic Equation | |
|---|---|---|
| Sutherland (1905) | $D = \dfrac{k_B T}{4\pi\mu R_o}$ | (4.3.9) |
| Glasstone et al. (1941) | $D = \dfrac{k_B T}{2\pi\mu R_o}$ | (4.3.10) |
| Scheibel (1954) | $D = \dfrac{AT}{\mu(\overline{V}_1)^{1/3}}\left[1+\left(\dfrac{3\widetilde{V}_2}{\widetilde{V}_1}\right)^{2/3}\right]$ | (4.3.11) |
| Wilke and Chang (1955) | $D = \dfrac{7.4\times10^{-8}(\phi\widetilde{M}_2)^{1/2}T}{\mu\overline{V}_1^{0.6}}$ | (4.3.12) |

Table 4.7 Theoretical estimations of TNT diffusion coefficients ($cm^2$/sec) for different temperatures

| Reference | T=20$^o$C | T=50$^o$C | T=80$^o$C |
|---|---|---|---|
| Stokes-Einstein | 0.63 x 10$^{-5}$ | 1.27 x 10$^{-5}$ | 2.13 x 10$^{-5}$ |
| Sutherland | 0.95 x 10$^{-5}$ | 1.90 x 10$^{-5}$ | 3.20 x 10$^{-5}$ |
| Glassstone | 1.89 x 10$^{-5}$ | 2.53 x 10$^{-5}$ | 6.40 x 10$^{-5}$ |
| Scheibel | 0.72 x 10$^{-5}$ | 1.44 x 10$^{-5}$ | 2.21 x 10$^{-5}$ |
| Wilke-Chang | 0.72 x 10$^{-5}$ | 1.45 x 10$^{-5}$ | 2.44 x 10$^{-5}$ |

# CHAPTER 5

# MODELING FOR SINGLE PARTICLE

## 5.1 Introduction

Every conceptual picture or model for the progress of reaction comes with its mathematical representation, its rate equation, and vice versa. If a model corresponds closely to what really takes place, its rate expression will closely predict the actual kinetics; if a model widely differs from reality, then its kinetic expressions will be of limited value. The requirement for a good engineering model is that it should be a close representation of reality, which can be used without too many mathematical complexities. The physical description of the target system is fundamental. A whole and clear description can make the model closer to the real world and may provide better results. TNT in the environment, which was discussed in Chapter 2, is often found in solid (crystal) form. In addition, bulk explosives, which need to be destroyed, are usually stored in solid form. If the TNT is destroyed using alkaline hydrolysis, the reactions must be carried out in aquatic media. Hence, heterogeneous and homogeneous reactions both have to be considered when modeling destruction of explosives.

TNT alkaline hydrolysis must modeled with heterogeneous and homogeneous reactions. In practice, imagine a spherical TNT particle reacts in NaOH media; initially, the reaction only occurs on the particle surface, and this initial reaction is best modeled as heterogeneous. The situation where TNT dissolves and then reacts in solution is

homogenous.

$$\left(\frac{\text{reaction rate}}{\text{particle area}}\right) = \kappa_1 \left(\begin{array}{l}\text{OH concentration}\\ \text{on the surface}\end{array}\right)$$

Here $\kappa_1$ is the heterogeneous rate constant, and its dimension is length per time, the same as the mass transfer coefficient,

As the reaction proceeds, the particle becomes porous and the chemical reaction may occur not only at the surface but on pore surfaces throughout the particle. In some cases, the pore area may far exceed the particle's superficial surface area (Cussler, 1997). The reaction may be modeled as homogeneous, as follows:

$$\left(\frac{\text{reaction rate}}{\text{particle volume}}\right) = \kappa_2 \left(\begin{array}{l}\text{TNT concentration}\\ \text{per volume}\end{array}\right)$$

$\kappa_2$ is the reaction constant. Thus the reaction of TNT particles can be modeled as heterogeneous or homogeneous. The choice of a model for the reaction is often subjective, and reasons for choosing the method are rarely stated in the literature. Therefore the approach for modeling the reaction process of TNT hydrolysis will be to use several different fundamental assumptions, and the appropriate adaptation of model will be determined in future.

Model verification will not be performed because the amount of TNT needed would exceed the permitted amount in our laboratory. Model verification is left for others who have access to the appropriate facility.

**5.2 Single Particle with Heterogeneous Reaction**

The shrinking particle model is used to describe situations in which solid particles are consumed either by dissolution or reaction and finally disappear. This model applies to fields ranging from pharmacokinetics to the formation of an ash layer around a burning coal particle (Fogler, 1992).

The end-products and intermediates in the TNT-alkaline hydrolysis reaction are not in solid form. Therefore the shrinking particle model is the first approach investigated. It is critical to know what resistance controls the reaction rate. Reactions like these are said to be diffusion-controlled when the diffusion steps take much longer than the reaction steps.

For simplification, we assume a single rigid sphere without pores with a first-order, irreversible reaction. The overall reaction rate is diffusion controlled through a liquid film. Figure 5.1 shows our modeling system.

As illustrating in Figure 5.2, the overall reaction process can be described as 1. $OH^-$ diffuses through the liquid film to the TNT particle surface. 2. Reaction of $OH^-$ and TNT occurs on the particle surface. 3. Diffusion of the end products from the solid surface through the liquid film back to the bulk solution.

Helimann et al (1996) suggested an E-2 elimination mechanism for RDX and HMX. Prisley (1998) also perform a series of TNT alkaline hydrolysis experiments. The transform efficiency of TNT to NaOH is 1.4 g TNT/g NaOH (3.3g TNT/g $OH^-$) within four hours at temperatures ranging from 60 - 100 °C to a non-energetic substance (Fraunhofer *et al*, 1995).

When the outside diffusion rate of a shrinking particle is the rate-controlling mechanism, the key variable becomes the mass transfer coefficient. The mass transfer coefficient is often a function of particle size. To develop the heterogeneous model, some assumption should be applied:

1. Reaction on the TNT particle surface proceed very fast, therefore, OH⁻ concentration is zero there ($C_{OH, s}=0$)

2. If the overall reaction rated is controlled by the mass transfer of OH⁻

$$\frac{dMass_{OH}}{dt} = KA(C_{OH} - C_{OH,s})$$ (5.2.1)

Applying the stoichiometry of TNT and OH⁻ (3.3g/g), the reaction becomes

$$\frac{dMass_{OH}}{dt} = 3.3(\frac{dMass_{TNT}}{dt})$$ (5.2.2)

Calculating the rate of TNT consumption as a function of particle size

$$Mass_{TNT} = \frac{4}{3}\pi r^3 \rho_{TNT}$$ (5.2.3)

Substituting equation 5.2.3 to 5.2.2 and 5.2.1 the rate becomes:

$$\frac{d(\frac{4}{3}\pi r^3 \rho_{TNT})}{dt} = 4\pi r^2 K C_{OH}$$ (5.2.4)

This reaction can be divided into different cases, as follows:

Case 1. Small particle size in Stokes Region (Levenspiel, 1972):

The mass transfer coefficient K is

$$K = \frac{D_{OH}}{r}$$ (5.2.5)

$D_{OH}$ is diffusion coefficient of OH⁻, substitute the mass transfer coefficient to eqn. 5.2.4

$$\frac{dr}{dt} = 3.3\left(\frac{D_{OH}C_{OH}}{r\rho_{TNT}}\right) \tag{5.2.6}$$

Integrating the eqn 5.2.6, and substituting the initial particle radius $R_0$

$$r^2 = R_0^2 - 6.6\left(\frac{D_{OH}C_{OH}}{\rho_{TNT}}\right)t \tag{5.2.7}$$

Case 2: Large particle with forced convection:

The case can be developed by considering forced convection of NaOH media around TNT spheres (Levenspiel, 1972), as follows:

$$\frac{Kd}{D_{OH}} = 2.0 + 0.6\left(\frac{dv}{\upsilon}\right)^{1/2}\left(\frac{\upsilon}{D_{OH}}\right)^{1/3} \tag{5.2.8}$$

$v$ is fluid velocity and $\upsilon$ is the kinematic viscosity. $d$ is TNT particle diameter.

For fluid motion to become insignificant the viscosity terms much approach zero. In practical systems, it is very difficult to reach $(Kd/D_{OH})=2$ experimentally.

The mass transfer coefficient K

$$K = \left(\frac{0.42v^{1/2}D_{OH}^{2/3}}{\upsilon^{1/6}}\right)\left(\frac{1}{r^{1/2}}\right) \tag{5.2.9}$$

Substitute the equation 5.2.9 to equation 5.2.4

$$r^{3/2} = R_0^{3/2} - 2.10\left(\frac{v^{1/2}D_{OH}^{2/3}}{\upsilon^{1/6}}\right)\left(\frac{C_{OH}}{\rho_{TNT}}\right)t \tag{5.2.10}$$

Case 3: Large particle with free convection due to gravity change:

$$\frac{Kd}{D_{OH}} = 2.0 + 0.6\left(\frac{d^3\Delta\rho g}{\rho\upsilon^2}\right)^{1/4}\left(\frac{\upsilon}{D_{OH}}\right)^{1/3} \tag{5.2.11}$$

The mass transfer coefficient K

$$K = \left( \frac{0.50 \Delta \rho^{1/4} g^{1/4} D_{OH}^{2/3}}{\rho_{TNT}^{1/4} \upsilon^{1/6}} \right) \left( \frac{1}{r^{1/4}} \right) \qquad (5.2.12)$$

In this case, the $\Delta\rho$ is the density difference of saturated TNT solution (boundary condition) and the density of reaction media (NaOH). However due to the low solubility of TNT, the density difference is not enough to cause the convection. The case is generally applied when high temperature variation or the gas-solid phase reaction, causes significant density change.

OH⁻

OH⁻

OH⁻

Reaction occurs on
TNT particle surface
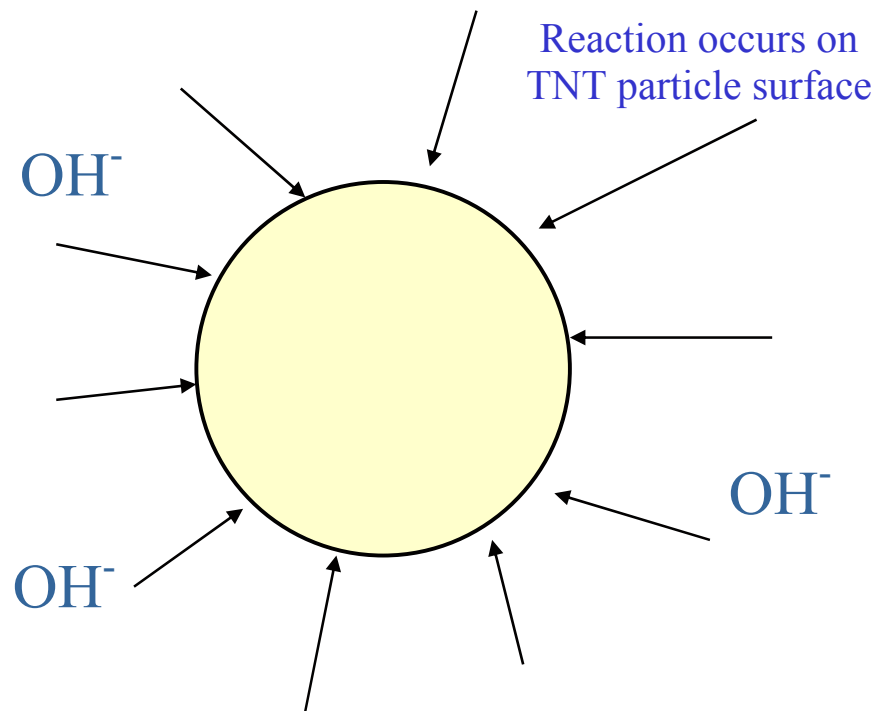
Figure 5.1 Shrinking particle model for TNT alkaline hydrolysis
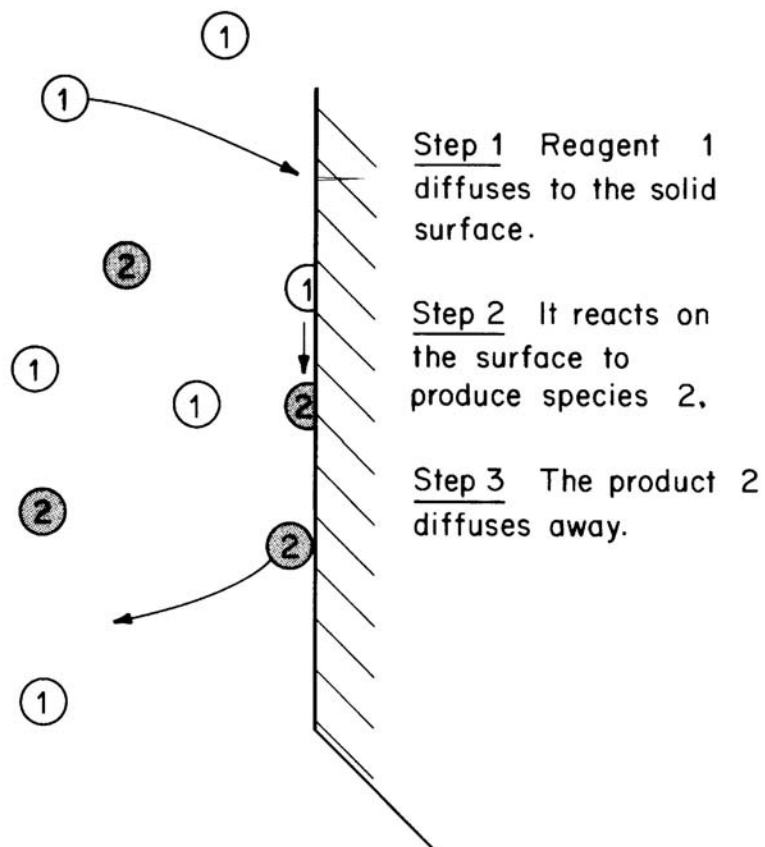
Figure 5.2 Diffusion and heterogeneous reaction. The reaction is irreversible and the overall reaction rate depends on the sum of resistances. (Cussler, 1997)

**5.3 Results**

The previously discussed models were used to develop closed form solutions for modeling TNT particles. They were ordered according to size. Equation 5.2.5 is used to obtain the equation 5.3.1 for the small particles.

$$r = \sqrt{R_0{}^2 - 6.6\left(\frac{D_{OH}C_{OH}}{r\rho_{TNT}}\right)t}$$

(5.3.1)

This equation would apply to particles of 0.2 cm radius. Typical alkaline hydrolysis for this equation would be pH=11.5 (OH⁻ concentration=6.5mM/L=0.11g/L), 20°C, and OH⁻ diffusivity of $5.28 \times 10^{-5}$ cm/s² (CRC Handbook, 1997). TNT density is 1.654 g/cm³ at 20°C. Substituting these conditions into equation 5.3.1 produces the results shown in Figure 5.3. The particle radius decreases 4% after 2000 minutes.

For large particles with forced convection, equation 5.2.10 can be rearranged as shown in equation 5.3.2.

$$r = \left[R_0{}^{3/2} - 2.10\left(\frac{v^{1/2}D^{2/3}}{\upsilon^{1/6}}\right)\left(\frac{C_{OH}}{\rho_{TNT}}\right)t\right]^{2/3}$$

(5.3.2)

Figure 5.4 shows the results for a particle of 1 cm radius with 1cm/s fluid velocity. The viscosity of water is about 1centipoise, The kinematics viscosity of aquatic solution is close to water (0.01 cm²/s). The particle radius decreases 3% after 2000 minutes.

**5.4 Single Sphere without Stirring (Homogeneous Reaction)**

The previous cases described the heterogeneous reaction which only occurs on the surface of the particle. In this section, we examine the homogenous reaction, where only the TNT which diffuses from the particle surface can react. Figure 5.5 shows the

homogeneous reaction system. The modeling approach is to develop a mass balance around the shell as follows:

$$\begin{pmatrix} \text{solute accu.} \\ \text{within the shell} \end{pmatrix} = \begin{pmatrix} \text{diffusion} \\ \text{into the shell} \end{pmatrix} - \begin{pmatrix} \text{diffusion} \\ \text{out the shell} \end{pmatrix} - \begin{pmatrix} \text{reaction} \end{pmatrix}$$

Equation 5.4.1 is the mass balance:

$$\frac{\partial}{\partial t}(4\pi r^2 \Delta r C) = \left[4\pi r^2 j\right]_r - \left[4\pi r^2 j\right]_{r+\Delta r} - rxn \tag{5.4.1}$$

By applying Fick's Law in spherical coordinates with constant diffusion coefficient and density, and combining with the reaction term, we get

$$\frac{\partial C}{\partial t} = \frac{D}{r^2}\frac{\partial}{\partial r}\left(r^2 \frac{\partial C}{\partial r}\right) - rxn \tag{5.4.2}$$

with $rxn = kC_{TNT}C_{OH}$ equation 5.4.2 becomes

$$\frac{\partial C_{TNT}}{\partial t} = \frac{D_{TNT}}{r^2}\frac{\partial}{\partial r}\left(r^2 \frac{\partial C_{TNT}}{\partial r}\right) - kC_{TNT}C_{OH} \tag{5.4.3}$$

subject the following boundary conditions

$$r = R_0 \quad C_{TNT} = C_{TNT}^{sat} \tag{5.4.4}$$

$$r = \infty \quad C_{TNT} = 0 \tag{5.4.5}$$

This equation can be solved numerically using finite differences (FDM) with Matlab (Mathworks Inc, Natick, MA) the Crank-Nicolson (Davis, 1984), (Borse, 1997) finite difference method (FDM). The Matlab program is in Appendix.

## 5.5 Results

The reaction conditions are essentially the same as the heterogeneous reaction. The particle radius is assumed to be 0.2 cm. The diffusion coefficient of TNT is $7.4 \times 10^{-6}$ cm/s$^2$ (see Chapter 4, using estimated result). The reaction environment is in pH=11.5 (OH$^-$ concentration is 6.5mM/L) at 20$^o$C. The TNT concentration is assumed to be saturated at the surface of particle or 130mg/L (0.57mM/L). To facilitate finite difference solution, the differential operator in equation 5.4.3 is expanded as follows:

$$\frac{\partial C_{TNT}}{\partial t} = D_{TNT} \frac{\partial^2 C_{TNT}}{\partial r^2} + \frac{2D_{TNT}}{r}\left(\frac{\partial C_{TNT}}{\partial r}\right) - kC_{TNT}C_{OH} \qquad (5.5.1)$$

If OH$^-$ is in excess, we can assume $C_{OH}$ is constant the reaction rate is pseudo-first-order, with the reaction constant $K_{OH}=kC_{OH}$, The value at 20$^o$C is 0.00835 min$^{-1}$ (Priestley, 1998).

The following boundary conditions were used.

$$r = R_0 \quad C_{TNT} = 130 \text{ mg/L} \qquad (5.5.2)$$

$$r = \infty \quad C_{TNT} = 0 \qquad (5.5.3)$$

To avoid a singularity at r = 0 (Browning, 1988), points are shifted from the boundary, (Swarztrauber, 1996). Figure 5.6 shows the concentration profile as a function of distance for various time intervals. The maximum reaction time in this model is 2000 minutes.

To relate the amount reacted in Figure 5.6 to particle radius, a second balance must be performed. The mass of reacted TNT is calculated from the flux at each time step and used to determine the new particle radius, as follows:

$$\frac{dM}{dt} = -Area * Flux = -Area * D\frac{dC}{dr}\bigg|_{r=0} \tag{5.5.4}$$

The particles are spherical, which means the $M = \rho * \frac{4}{3}\pi r^3$ and $A = 4\pi r^2$. Therefore the change in radius is calculated using equation 5.5.5.

$$\frac{dr}{dt} = -\frac{D}{\rho}\frac{dC}{dr}\bigg|_{r=0} \tag{5.5.5}$$

The new flux was calculated in each time step in the Matlab simulation using the gradient surface gradient. This results in an ordinary differential equation, which is solved using Euler's method. Figure 5.7 shows the flux change over time. Figure 5.8 shows the particle radius change over time. The shrink rate is slow, about 1% of particle radius for 2000 minutes. The low solubility (130mg/L) of TNT contributes to the lengthy time for reaction.

By comparing the modeling results with heterogeneous and homogenous reactions applied for particle in Stoke's region, shown in Figure 5.9. The importance of the differences in assumptions can be observed. The homogenous model predicts slower particle shrink rate than the heterogeneous particle, however, the reaction time in the same order of magnitude. The reasons may be: 1. Both overall reaction rates are limited by diffusion. In the heterogeneous model, OH⁻ limits the overall reaction rate. In

homogeneous model, TNT limits the overall reaction rate. 2. Since both overall reaction rates are limited by diffusion, and OH⁻ has higher diffusion coefficient than TNT. Therefore heterogeneous reaction shows faster reaction time. 3. Heterogeneous model eliminates the time for surface reaction.

## 5.6 Porous Catalyst Model (Pseudo-homogeneous)

This model has been applied in modeling activated sludge process (Stenstrom and Song, 1991). The effect of this diffusion and reaction process on intrinsic reaction is summarized in terms of global reaction rates. By envisioning that these global rates occur homogeneously throughout the reactor volume, homogeneous modeling techniques are then applied to the reactor. In extensive literature on the modeling of heterogeneous chemical reactions, the extent of mass transport limitation in porous catalyst is often characterized by two dimensionless parameters, the Biot number and the Thiele modulus. The Biot number (*Bi)* characterized the influence of the external resistance.

$$Bi = \frac{KL}{D_e} \qquad (5.6.1)$$

where $K$ is mass transfer coefficient referenced in Section 5.3. $L$ is characteristic dimension, and $D_e$ is the effective diffusivity in the porous solid phase.

The Biot number is the ratio of the characteristic time for diffusion across the porous particle to the characteristic time for diffusion across the boundary between the fluid phase and the particle surface. Hence, transport limitation is dominated by external resistance when this ratio is small.

By using realistic values of mass transport parameters, the external mass transport limitation, cannot exist without the presence of internal mass transfer limitation. The influence of internal resistance, which is the resistance of the particle matrices, is characterized by the Thiele modulus ($\phi$).

$$\phi^2 = \frac{L^2 \overline{R}}{D_e c_B}$$

(5.6.2)

where $\overline{R}$ is the intrinsic rate of reaction, $c_B$ is the concentration of the reactant in the bulk fluid.

This modulus can be interpreted as being the ratio of the characteristic time for diffusion to the characteristic time for reaction. Alternately, it can be interpreted as the ratio of the intrinsic rate of reaction to the maximum rate of diffusion. Hence, the extent to which internal mass transport limitation is significant depends on the relative rates of reaction and diffusion.

The effectiveness factor $\eta$ (Thiele, 1939) is defined as follows:

$$\eta = \frac{\left(Rate_{actural}\right)}{\left(Rate_{no.diffusion}\right)}$$

It is also suggested that if $\phi$ is small (or $\phi < 0.5$) $\eta \sim 1$, the resistance can be neglect if $\phi$ is large (or $\phi > 5$), $\eta = 1/\phi$.

The Biot number and Thiele modulus account for particle geometry through the characteristic length parameter L.  The characteristic length is sometimes defined to be the ratio of the bulk volume of the particle (solid plus void volume) to the external

surface area of the particle. The first advantage is that it avoids the difficulty of determining the mean size for the highly irregular shape of TNT particles. The second advantage is that the effect of particle shape on the relationship between the Thiele modulus and the effectiveness factor is minimized. Although particle shape is not expected to be an important consideration, a specific geometry is needed for facilitate the derivation of the model equations. The following derivation begins with spherical geometry and then generalizes to include cylindrical and slab geometries. The derived equation is a mathematical description of the concentration distribution of a reactant as it diffuses through a particle. Figure 5.6 illustrates the spherical particle of radius $R_0$ applied in this model.

Assume a mass balance of the spherical shell and apply Fick's Law as follows.

$$\frac{\partial C_{TNT}}{\partial t} = \frac{D_{e,TNT}}{r^2} \frac{\partial}{\partial r}\left(r^2 \frac{\partial C_{TNT}}{\partial r}\right) - kC_{TNT}C_{OH} \qquad (5.6.3)$$

This equation is similar to equation 5.4.2. However, the boundary conditions are different, as follows:

$$r = 0 \qquad \frac{dc_{TNT}}{dr} = 0 \qquad (5.6.4)$$

$$r = R_0 \qquad D_{e,TNT}\frac{dc_{TNT}}{dr} = K(C_{TNT} - c_{TNT}) \qquad (5.6.5)$$

where $C_{TNT}$ is concentration of TNT in bulk liquid, $c_{TNT}$ is concentration of TNT inside particle, and $K$ is mass transfer coefficient.

This model can be solved using FDM with Matlab in a fashion similar to equation 5.5.1. This model is not solved in this dissertation and is left for future investigators.
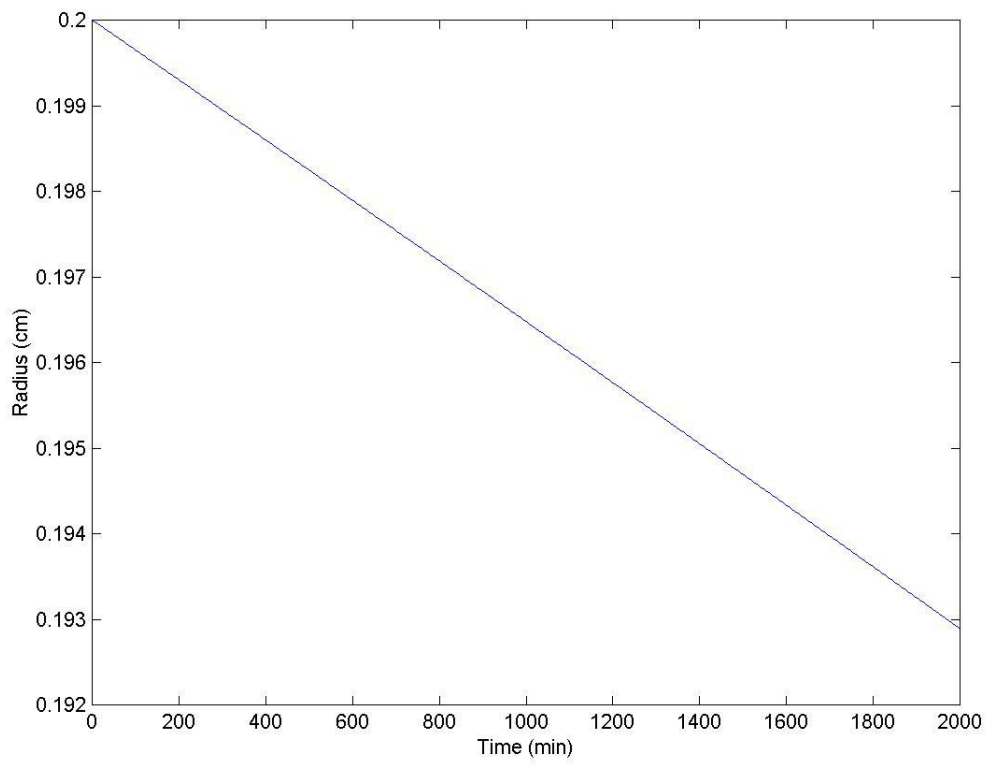
Figure 5.3  Modeling result of small TNT particle (radius 0.2cm).
Shrink with time.
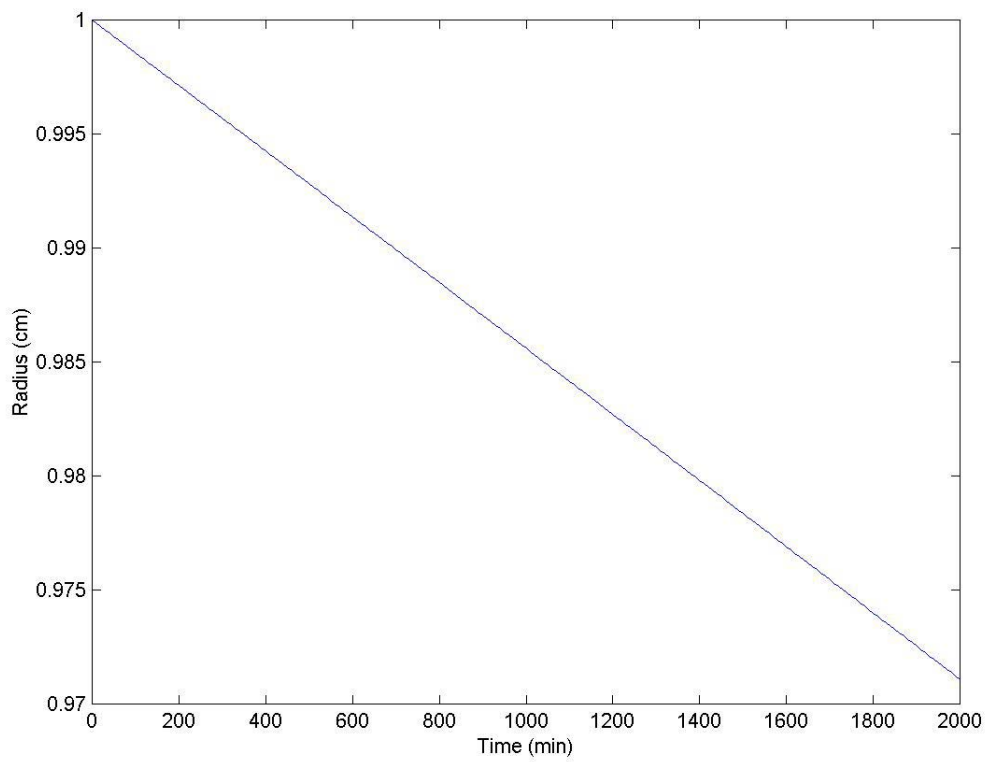
Figure 5.4 Modeling result of large TNT particle (radius 1cm) with
forced convection velocity 1cm/s (60cm/min)

OH⁻

OH⁻

TNT

TNT

OH⁻

TNT

OH⁻

**TNT dissolves and reacts in solution**
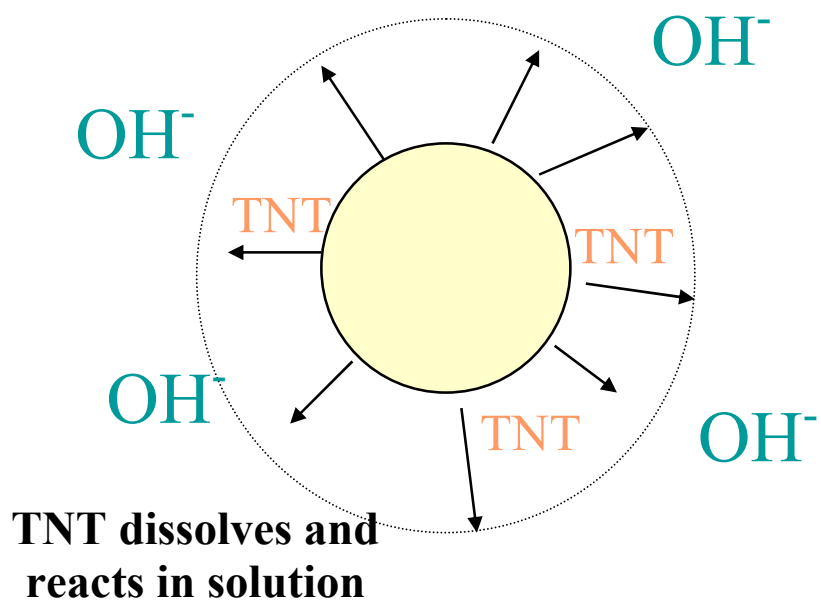
Figure 5.5 Homogeneous reaction system for TNT alkaline hydrolysis
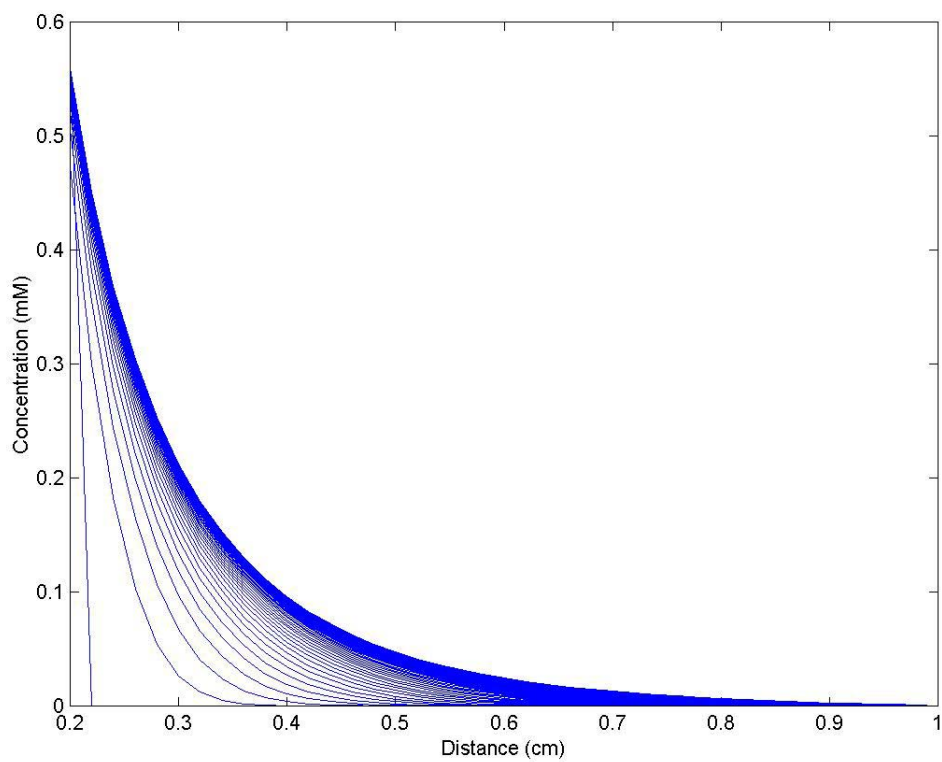
Figure 5.6 Modeling result of homogeneous reaction. The maximum reaction time in this model is 2000 minutes. Particle radius was 0.2cm.
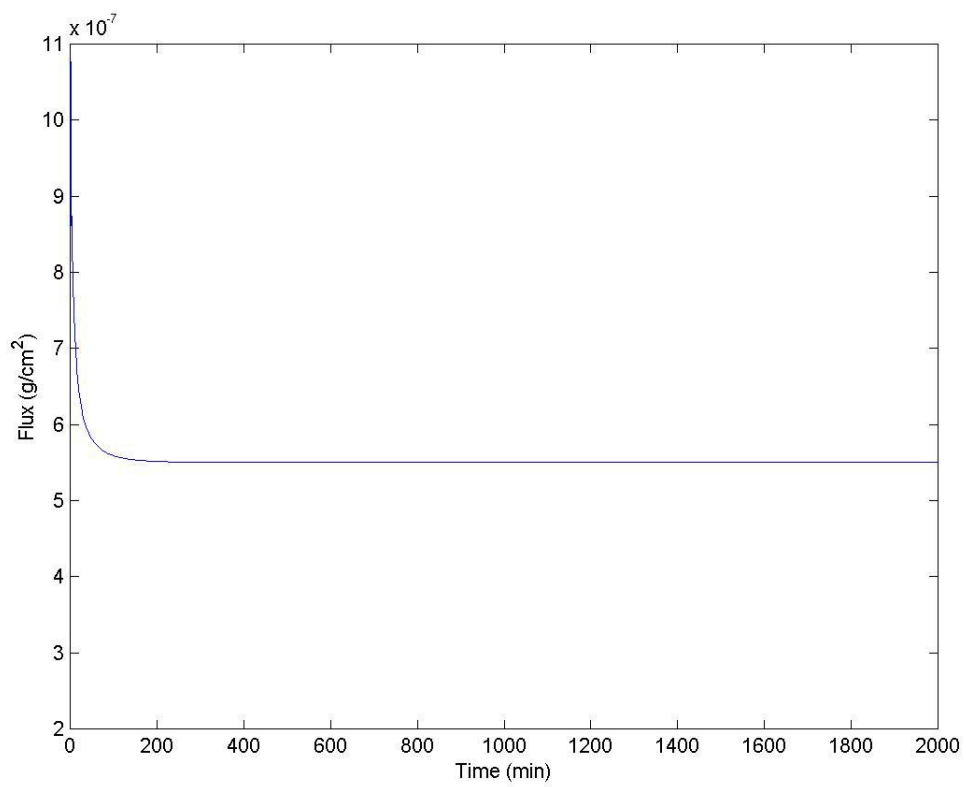
Figure 5.7 TNT flux versus time. The flux was calculated from the concentration gradient on the surface of the particle. The maximum reaction time in this model is 2000 minutes.
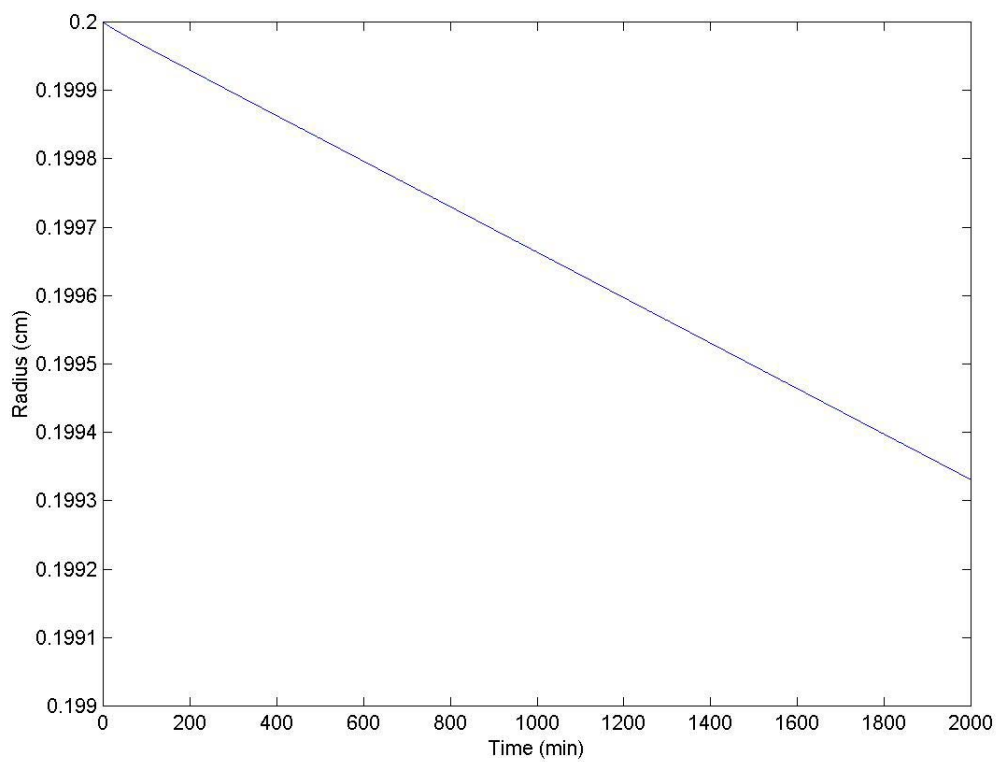
Figure 5.8 Particle radius decreases with time. The reaction time applied homogeneous model is 2000 minutes. However, particle size is still over 0.199 cm, the reaction rate is slow.
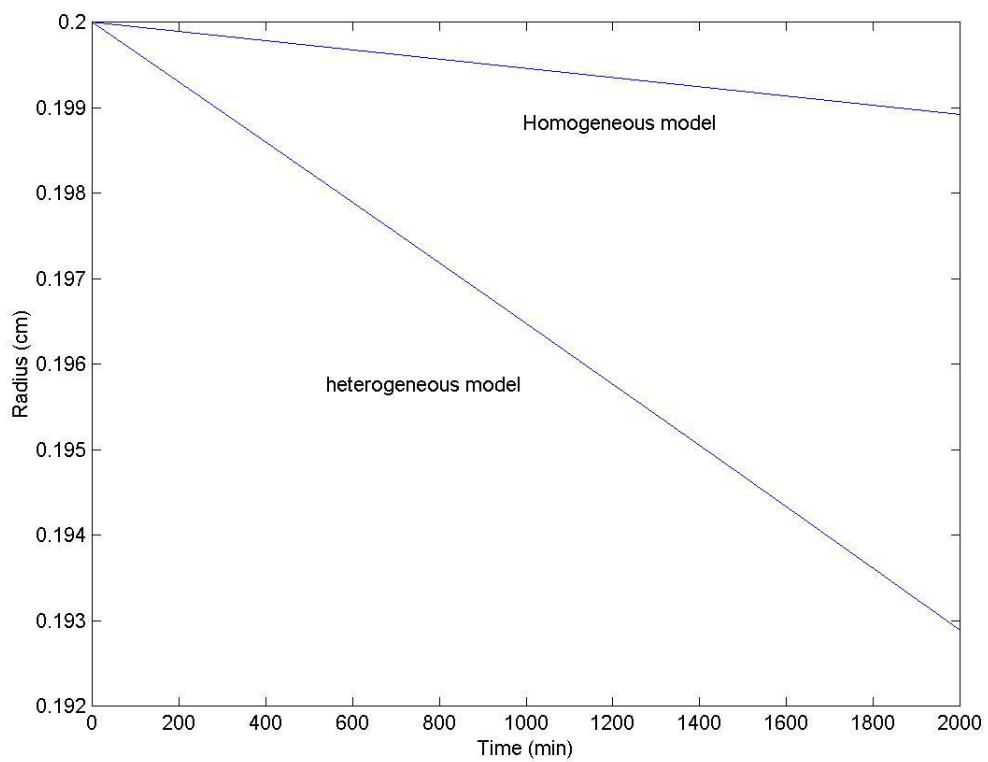
Figure 5.9  Comparing the modeling results with heterogeneous
and homogenous reactions applied for particle in
Stoke's region,

# CHAPTER 6

# MODELING OF MULTIPLE PARTICLES

## 6.1 Introduction

In modeling the treatment processes, particle size is an important factor. Bulk explosives in solid form show great heterogeneity of particle size. The particles are never uniform; hence, particle size distribution, or the size of a single particle is also needed. Most particulate systems, which are of practical interest, have a wide range of particle sizes, and it is necessary to quantitatively know the mean and distribution of sizes. The mean size can most conveniently be represented using a cumulative mass fraction curve; the proportion of particles (x) smaller than a certain size (d) is plotted against that size (d). A typical curve for size distribution on a cumulative basis is shown in Figure 6.1 (top, Coulson *et. al*, 1991).

The distribution of particle sizes can be seen more readily by plotting a size frequency curve, such as that shown in Figure 6.1 (bottom, Coulson *et. al*, 1991) in which the slope (dx/dd) of the cumulative curve is plotted against particle size (d). The most frequently occurring size is shown by the maximum of the curve. For naturally occurring materials the curve will generally have a single peak. For mixtures of particles, there may be as many peaks as components in the mixture.

The frequency curve is more useful for modeling TNT treatment, because it is necessary to know how many particles or how many percentage of a certain size. Sieving is often used to determine the particle size distribution. To obtain an accurate size

distribution it is necessary to have a large number of particles. This is difficult to do with explosives since the required mass of particles may be hazardous, requiring handling in special facilities. Generally our laboratory is limited to 1 gram or less of TNT, which makes it difficult to experimentally determine particle size and distribution. In the absence of experimentally determined information, an ideal distribution such as a Gaussian distribution is often assumed as the frequency curve of TNT particles.

## 6.2 TNT Particle Size Characteristics

TNT used in industrial or military applications is not in homologous form; TNT is a collection of yellow monoclinic crystals, which are irregularly shaped. In Chapter 5, the TNT alkaline hydrolysis was modeled as a single spherical particle, which was required to facilitate the mathematics. The sphere is the simplest particle shape and orientation does not need to be considered due to its symmetry. To extend this concept to irregularly shaped particles, the size is defined in terms of the size of an equivalent sphere. However, the particle is represented by a sphere of different size according to the property selected. Some of the important sizes of equivalent spheres are as follows:

(a) The sphere of the same volume as the particle.

(b) The sphere of the same surface area as the particle.

(c) The sphere of the same surface area per unit volume as the particle

(d) The sphere of the same area as the particle when projected on to a plane perpendicular to its direction of motion.

(e) The sphere of the same projected area as the particle, as viewed from above, when lying in its position of maximum stability.

(f) The sphere which will just pass through the same size of square aperture as the particle, as on a screen.

(g) The sphere with the same settling velocity as the particle in a specified fluid (Coulson, 1991).".

Several of the above definitions depend on the measurement of a particle in a particular orientation, Thus, the statistical diameter (defined as Feret's diameter in Coulson, 1991) is the mean distance between two parallel lines which are tangent to the particle in an arbitrarily fixed direction, irrespective of the orientation of each particle observed. In effect the diameter is the greatest particle dimension.

A measure of a particle shape which is frequently used is the sphericity, $\psi$, defined as the surface area of a sphere equal in volume to the particle divided by the actual particle surface area.

## 6.3 TNT Particle Size Distribution

Particle size distribution of our TNT sample (obtained from Lawrence Livermore National Laboratory in 1997) was obtained using a stereo microscope (Leica – model number MZ12 using a reticule at 10 power). Figure 6.2 shows TNT particles. The TNT particles are in the monoclinic form, which is more stable. Approximately 200 particles were counted, and the average length and width were measured. The particles were counted by separating them into 10 groups. The data were pooled to produce a final count.

Table 6.1 and Figure 6.3 show the results, which is a double peak distribution. The double peak may be the result of a limited sample size.

## 6.3. Modeling for Multiple Particles

It is necessary to extend the single particle model to multiple particles to improve the model's utility and to apply it to actual applications of TNT alkaline hydrolysis. Several approaches are possible to model multiple particle systems. A single approach is developed here, but other approaches are discussed in Chapter 7.

If particles are dispersed, and $OH^-$ is in excess, it is possible to assume that there is no interaction or competition among particles. The particles can be divided into an arbitrary number of fractions based upon their size. Each size will contain a specific number of particles. The particles in each fraction will react independently of other fractions. As the reaction proceeds, the size of particles in each original fraction decreases, but the number of particles is constant. Finally, when all the mass reacts, the particles disappear, and the number in the particular fraction decreases to zero. As the simulation continues, the number of fractions decreases, until the largest particle-size fraction disappears. Using this approach, each fraction can be modeled as a single particle. Figure 6.4 shows the approach.

The total mass can be calculated from the mass of each particle and the particle distribution, as follows:

$$Mass_{particle} = \frac{4}{3}\pi r(t)^3 \qquad (6.3.1)$$

$$\text{Total Mass} = \sum_{\text{min}}^{\text{max}} Mass_{particle} \times Distribution(r) \tag{6.3.2}$$

The TNT distribution described in Table 6.1 was modeled in this fashion. The particles were modeled using five fractions, with distributions from 0 to 0.05 cm, 0.05 to 0.15 cm, 0.15 to 0.25 cm, 0.25 to 0.35 cm and 0.35 to 0.45 cm. The number of particles in each fraction was 36, 68, 58, 22, 6. Figure 6.5 shows the model result for heterogeneous reaction (equation 5.3.1). It should be noted that the particle size applied in the simulation is the diameter of the particle. The smallest particles disappear too quickly to be observed using the time scale used for the graph. By comparison, the largest particles take more than 2000 minutes to disappear although the particles in this fraction are only 3% of the total mass. It takes approximately 600 minutes for 50% of the mass to disappear.

The same TNT size distribution was also modeled with the homogeneous reaction (equation 5.4.3), in order to compare the heterogeneous reaction result. Figure 6.6 shows the modeling result applied homogeneous reaction. It takes much longer time to treat TNT particles with homogeneous reaction, as mentioned in previous chapter. The reaction time of the smallest particles (0.05 cm) is still not relevant in the time scale of the graph.

Particle diameter decreases rapidly in the beginning for the homogeneous model. After they decrease to approximate 80% of mass, the rate decreases. Particles with different sizes show large differences in time to complete the reaction, as observed in the

right end of the graph (t=20000 minutes). It is due to the low solubility of TNT in water, as discussed in Chapter 5.

In the beginning of simulation, flux is high and surface area is also large, and the mass decreases quickly. As the reaction proceeds, the particle diameter and surface area both decrease, reducing the reaction rate. This is in contrast to the heterogeneous model, where the shrink rate is less dependent to the surface area. The time to complete the reaction calculated by homogeneous reaction is 10 times greater than the time calculated by the heterogeneous reaction model.

The homogenous model can be used to investigate different particle size distributions, such as a Gaussian distribution. Any number of particle size fractions can be used. The difference in model time predictions to complete the reaction will increase as the particle size distribution becomes greater.

There are still other approaches. The case of particles interfering with each other will be discussed in the following chapter.
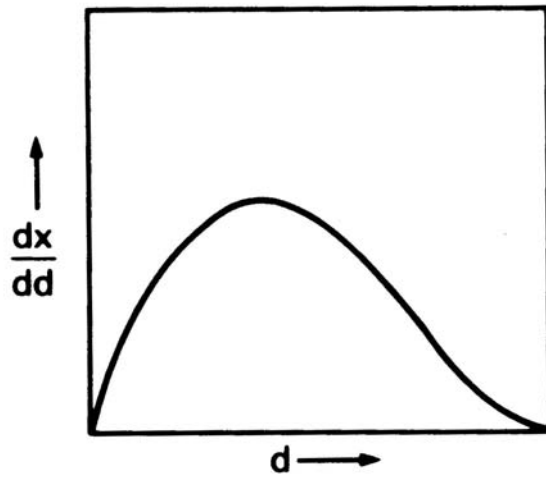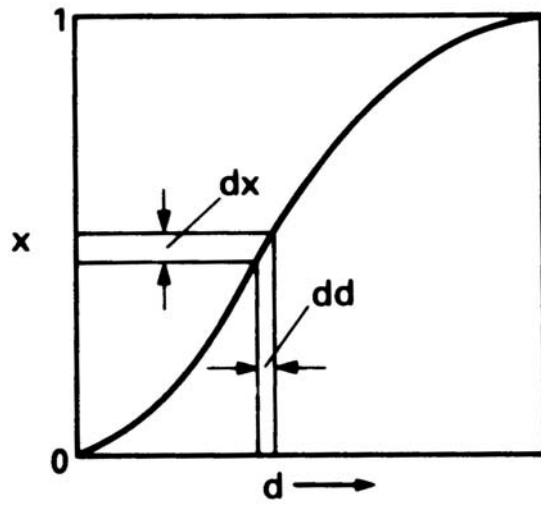
Figure 6.1a (above) A typical curve for size distribution on a cumulative basis.
Figure 6.1b (below) The slope (dx/dd) of the cumulative curve is plotted
against particle size (d). (From Coulson *et. al*, 1991)

87
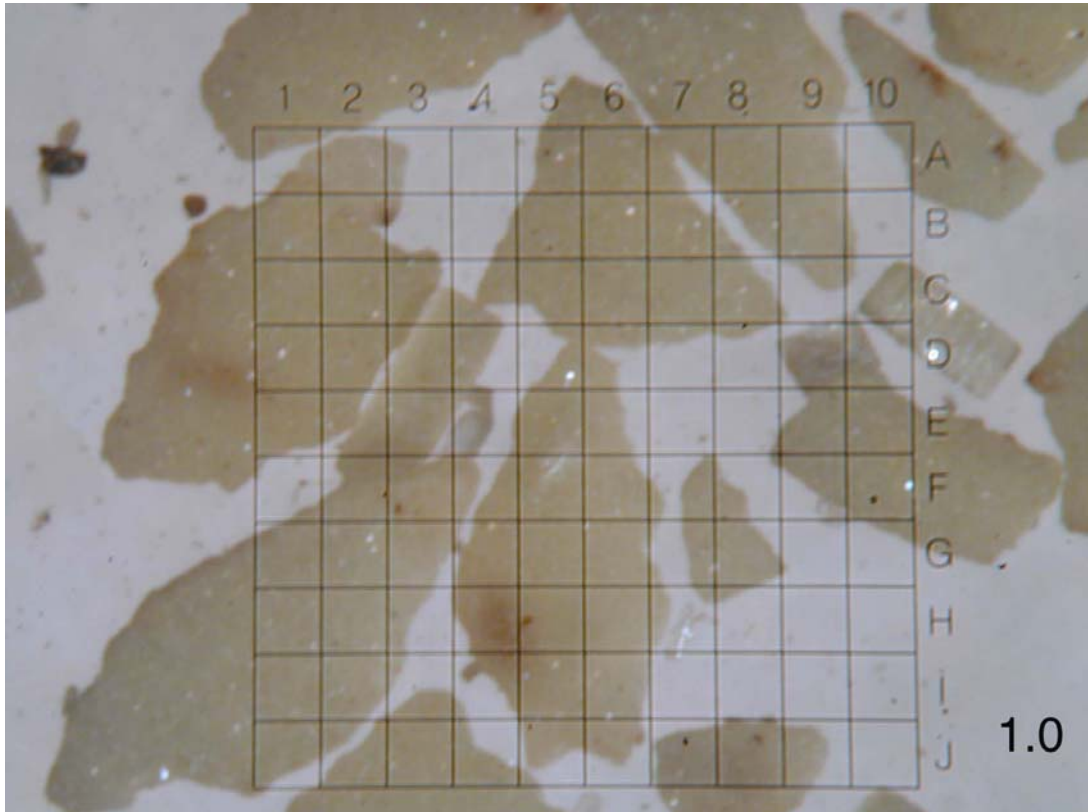
Figure 6.2. TNT particles looked through microscope (Leica
MZ12). 1.0x10 power.

Table 6.1 The TNT particle size distribution of our sample (size
determined by averaging the length and width.)

| grid | paticle size | number |
|------|--------------|--------|
| 1 | 0.05 | 36 |
| 2 | 0.10 | 41 |
| 3 | 0.15 | 27 |
| 4 | 0.2 | 23 |
| 5 | 0.25 | 35 |
| 6 | 0.30 | 16 |
| 7 | 0.35 | 6 |
| 8 | 0.40 | 4 |
| 9 | 0.45 | 2 |
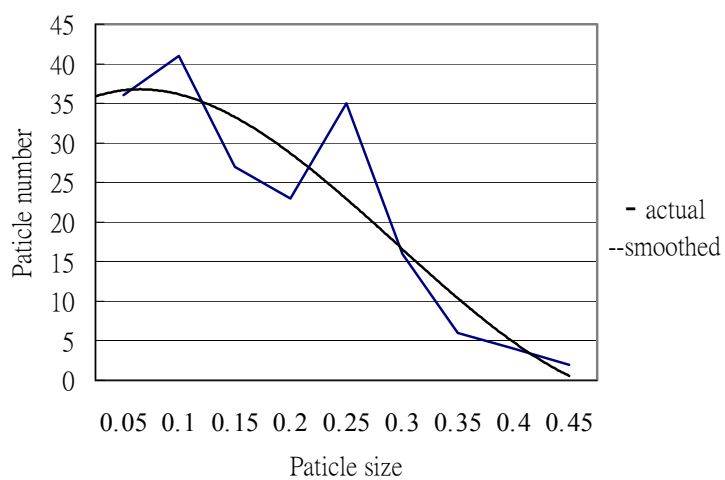


Figure 6.3 TNT particle size distribution, which shows a
double peak graph.
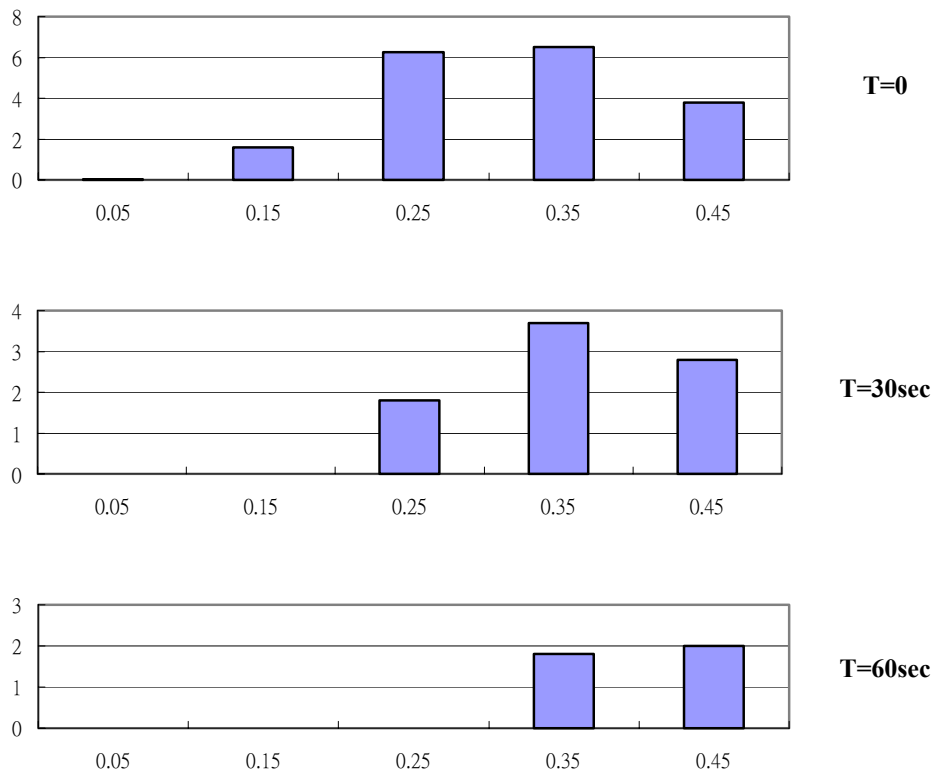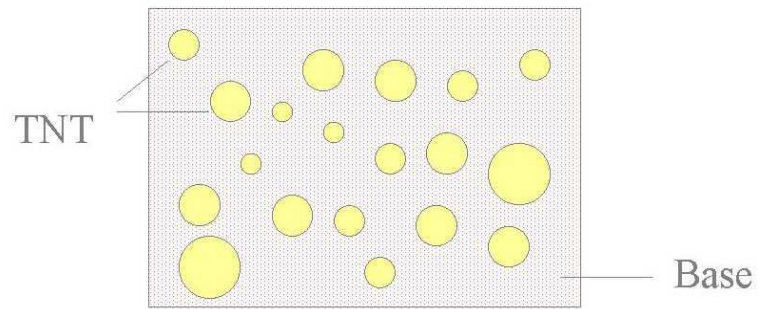
Figure 6.4a (above) Illustrations of modeling system. TNT are widely dispersed
　　　　　　in the system.
Figure 6.4b (below) Showing total mass fractions of TNT change with time.
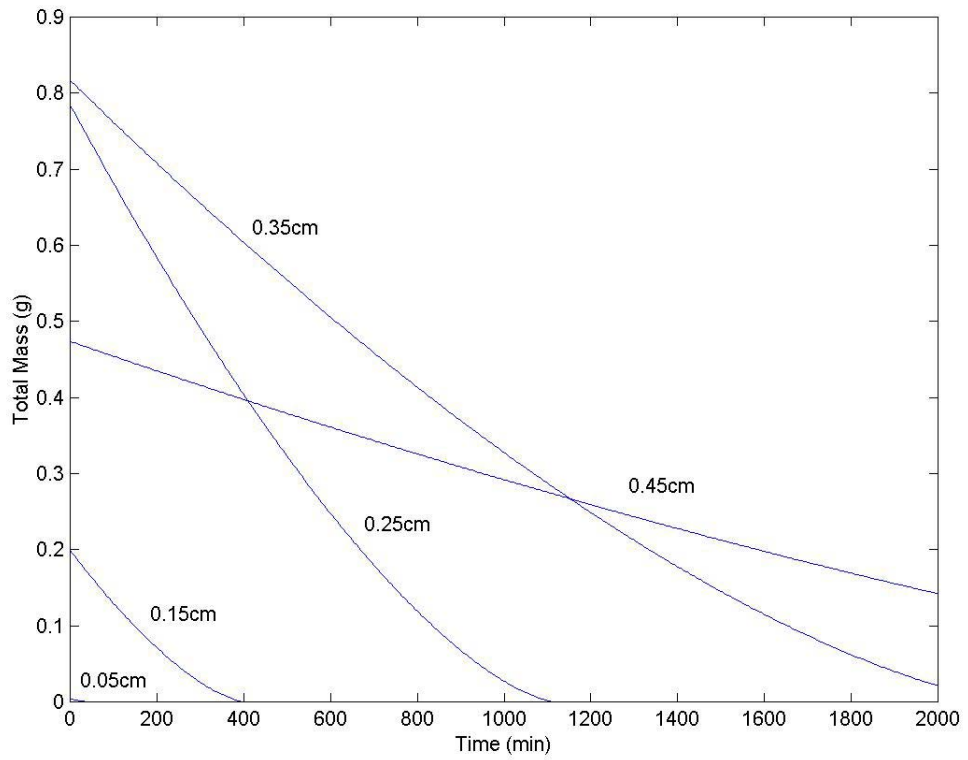
Figure 6.5 TNT mass as the function of time. The heterogeneous
reaction model was applied to calculate the radius
related with time.
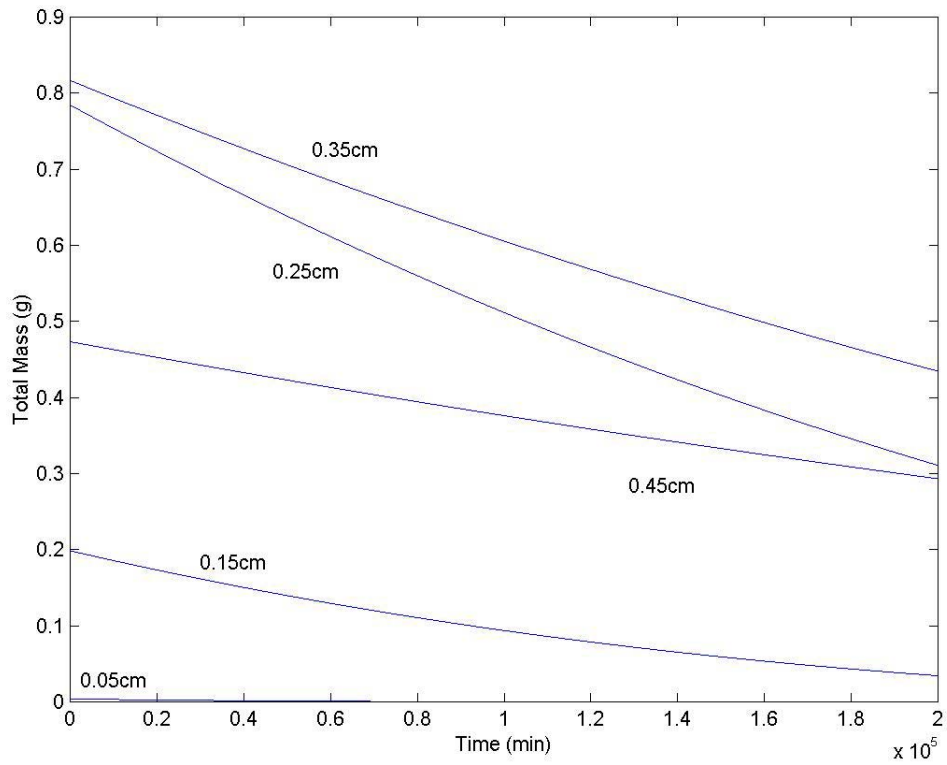
Figure 6.6 TNT mass as the function of time. The homogeneous
reaction model was applied to calculate the radius related
with time, the reaction time is $2 \times 10^5$ minutes.

# CHAPTER 7

# CONCLUSIONS AND FUTURE WORK

## 7.1 Introduction

This dissertation investigated the reaction of particulate TNT in a high pH solution, which is a process generally called alkaline hydrolysis. Alkaline hydrolysis has been used with success to treat non-aromatic explosives such as RDX and HMX. Diffusion coefficients were measured and used previously measured reaction rates to evaluate several modeling approaches. The modeling approaches differed because of different assumptions for TNT reaction. A homogenous model (TNT reacts in solution after it dissolves and diffuses from the surface) was evaluated using a numerical approach. This was compared to a heterogeneous model, which assumed that TNT reacts at the surface. Both appear to be diffusion controlled. The heterogeneous model predicts higher reaction rates.

This chapter also describes several future projects that will improve knowledge and extent the utility of the model. In addition to experimentally verifying the predictions from Chapters 5 and 6, additional modeling work can be performed. Also the approach can be extended to different materials.

**7.2 Single Sphere TNT Particle**

The shrinking sphere model (Levenspiel, 1972) was applied as first approach in modeling the TNT treatment process. Since the end products and intermediates are all soluble, the $OH^-$ diffuses to the surface and reacts with TNT molecules. Mass transfer is the rate-limiting step.   With an average TNT particle distribution (0.2cm for small particle, 1cm for large particle and convection speed 1cm/s), small particle radius decreased 4% and large particle radius decreased 3% over 2000 minutes of reaction time.

The other approach is the homogeneous reaction. This model assumes that the TNT dissolves in the reaction media first, and then diffuses out. The reaction occurs in the boundary layer. The relation must be described using partial differential equations. Using the Crank-Nicolson finite difference method, a particle with 0.2 cm  radius decreased 1% after 2000 minutes. Compared to the shrinking sphere particle model results, the homogeneous reaction model shows much slower rate due to the low solubility of TNT.

**7.3 Multiple Particle Model**

A more practical example is treatment of a group of particles. A sample of TNT was  manually counted to determine the size distribution, and the distribution was used in our model with five fractions.  It was assumed that the particles are independent and do not interfere with other particles, and OH is in excess. As the reaction proceeds, the size of particles in each original fraction decreases, but the number of particles is constant. The total mass of each fraction is added. With the shrinking sphere model, the largest particles take more than 2000 minutes to disappear. It takes 600 minutes to destroy 50%

of total mass. When modeling with homogeneous reaction, it takes much longer, as compared to the shrinking sphere particle model. Although particles radius decreases rapidly at the beginning of the reaction. It takes more than 20,000 minutes to finish the reaction. The convection effect may also be important, but was not included in the dissertation. It will be discussed in the future work.

The temperature for all the previously described results was 20$^o$C. A realistic industrial process would be operated at much higher temperature, perhaps as high as 90$^o$C. The time to destroy TNT would be dramatically decreased.

## 7.4 Future Work

### 7.4.1 Diffusion Coefficients

The experiments performed in this dissertation were limited to 20$^o$C, but is desirable extending the work to higher temperature, where hydrolysis reactions are more favorable (Heilman et al, 1996). To extend the work, it is necessary to measure diffusion coefficients in water over a range of elevated temperatures. Reactions coefficients are known at 50$^o$C and 80$^o$C (Priestly, 1998) but diffusion rates have not been measured. The first approach is to assume that the cell constant will not vary with the temperature. The second approach is to determine the cell constant as a function of temperature. Because there is currently no datum of diffusion coefficients of our standardization compounds (KCl, Phenol), the diffusion coefficients used in the calculation of cell constant $\beta$ should be estimated with Stokes-Einstein equations, or other empirical correlations. The membrane separating the two parts of the diffusion cell is an important factor in estimating the diffusion coefficients. The membrane properties may change with

the temperature. The second approach will be more closely related to the field applications.

RDX and HMX are frequently found with TNT. All three compounds can be used in the same explosive. Munitions plants frequently discharged them in the same wastewaters. Therefore a treatment technology that is effective for all three explosives would be useful. All three are ring compounds (RDX and HMX are non-aromatic) and have many similar properties. Extending the model to a mixture of RDX, HMX and TNT particles would be useful.

### 7.4.2 Modeling for Single Particle

The TNT samples provided by Lawrence Livermore National Laboratory have a large particle size distribution. The particle sizes vary from 0.05 cm to 0.5 cm. The particles are mostly fragments of large crystals. Adding shape factors (McCabe *et al*, 1985) to the model would enhance its utility. The use of spherical particles is the simplest approach. Forced convection also should be considered and the effect can be estimated with Peclet number. If Peclet is smaller than 1, the diffusion term in the equation is significant; if the Peclet number is larger than 1, the diffusion term can be neglected (Fogler, 1992).

The approach in this dissertation was restricted to constant temperature. Generally the destruction of explosives is performed in constant equipment for safety reasons. A non-isothermal porous catalyst model had been developed and applied (Aris, 1975) to other materials. Combining this approach with the approach in this dissertation might be useful, especially in understanding autothermal reactions. Reactor safety might be improved using such a model.

### 7.4.3 Modeling for Multiple Particles

The approach taken in this dissertation assumes no particle interaction. Therefore the concentration or concentration gradients of particles in suspension is unimportant. Alternative approaches that include particle interactions will further improve the model's utility to applications. Rowley (1994) suggested a "neighborhood" approach where a group of particles interact with each other. In this situation the OH will not be in excess, and the reaction cannot be treated as pseudo first-order. The neighborhood approach could be simplified by assuming the probability of particles merging into a neighborhood is equal to the chance of particle collision. The Leonard-Jones potential energy plane may be considered. The range of "neighborhood" may be defined as the lowest point in potential energy plane, which might be expressed as a function of particle size.

# APPENDIX

```
%this script solves the TNT particle size versus time
%with heterogeneous surface reaction described in Levenspiel book
%the particle size is in Stoke's region
%enter parameter here
%
%Diffusion coefficient of alkaline OH (cm^2/min)
Doh=5.28e-5*60;
%viscosity of water (g-cm/min)
vis=0.01*60;
%density of TNT particle (g/cm^3)
Ptnt=1.654;
%concentration of OH in bulk solution (g/cm^3)
Coh=0.1105*0.001;
%convection speed (cm/hr)
vel=0.1;
% Particle radius of TNT particle (cm)
Ro=0.2;
%Molecular weight of TNT
%MWtnt=227.16;
%
% reaction time and step
dt=5;
T=2000;
time=[0:dt:T]';
n=length(t);
%
%case 1 --small particle without convection
r1=(Ro^2*ones(n,1)-6.6*Doh*Coh/Ptnt*time).^0.5;
figure(4);clf
plot(time,r1)
```

```
%this script solves the TNT particle size versus time
%with heterogeneous surface reaction described in Levenspiel book
%the particle is large, with forced convection
%
%enter parameter here
%
%Diffusion coefficient of alkaline OH (cm^2/min)
Doh=5.28e-5*60;
%kinematic viscosity of water (cm^2/min)
vis=0.01*60;
%density of TNT particle (g/cm^3)
Ptnt=1.654;
%concentration of OH in bulk solution (g/cm^3)
Coh=0.1105*0.001;
%convection speed (cm/min)
vel=60;
% Particle radius of TNT particle (cm)
Ro=1;
%Molecular weight of TNT
%MWtnt=227.16;
%
% reaction time and step
dt=10;
T=2000;
t=[0:dt:T]';
n=length(t);
%
r2=(Ro^1.5*ones(n,1)-2.1001*vel^0.5*Doh^(2/3)/vis^(-1/6)*...
   Coh/Ptnt*t).^(2/3);
figure(2);clf
plot(t,r2);
```

```matlab
% This script is to solve a shinking ball
% with outside diffusion and homogeneous reaction
% dc/dt= D/r^2[d(r^2(dc/dr))/dr]
% As time goes by, the ball radius decrease
% but the boundary concentration remain the same
% also, it plots the flux with time
clear
% Enter parameter, those value is fixed
% diffusion coefficient (cm^2/min)
D=7.4383e-6*60;
% reaction const (1/min)
K=0.00835;
% boundary conditions (mM)
f0=0.57;
fR=0;
% TNT molecular weight
MWtnt=227.16;
%density of TNT particle (g/cm^3)
Ptnt=1.654;
% time step
dt=1;
T=2000;
time=[1:dt:T]';
R=1;
%RR=zeros(1,(T/dt))';
Rm=0.2;
%step size
dr=(R-Rm)/40;
%x-grid points
r=[Rm:dr:R]';
r1=[Rm:dr:R-dr]';
% Matrix size
n=length(r);
% Set initial concentration
C=zeros(1,n)';
% Transform into dimensionless form
DB=D*dt/dr^2;
KB=K*dt;
%
%Set 2nd Diffusion coeff as a function of r
rn=r/R;
rn1=r1/R;
VB=(D./rn)*(dt/dr);
VB1=(D./rn1)*(dt/dr);
DFC1=DB/2*ones(n-1,1)-VB1/2;
DFC2=DB/2*ones(n-1,1)+VB1/2;
%
%construct the matrices Ap(+DB) and Am(-DB)
%and to solve Ap*C=Am*C+b
Ap=sparse(diag((1+DB+KB/2)*ones(n,1))-...
   diag(DFC2,1)-...
   diag(DFC1,-1));
```

```matlab
Am=sparse(diag((1-DB-KB/2)*ones(n,1))+...
    diag(DFC2,1)+...
    diag(DFC1,-1));
%F=zeros(1,(T/dt)+1)';
RR(1,1)=0.2;
%Boundary condition set as vector b
C(1,1)=f0;
b=VB.*[f0 zeros(1,n-2) fR]'+DB*[f0 zeros(1,n-2) fR]';
figure(1),clf
plot(r,C);hold on
for t=1:dt:T
    C=Ap\(Am*C+b);
%calculate the flux, and change the units
    F(t/dt,1)=D*(C(1,1)-C(2,1))/dr*MWtnt*1e-6;
% calculate the particle radius with flux
    if t<T & RR(t/dt,1)>F(t/dt,1)*dt/Ptnt
    RR(t/dt+1,1)=RR(t/dt,1)-F(t/dt,1)*dt/Ptnt;
    end
    if mod(t,4)==0
    plot(r,C)
    end
end
hold off
figure(2),clf;
plot(time,F)
figure(3), clf;
plot(time,RR)
```

```matlab
% This script is to compare both models applied for
% a particle in Stoke's region
%
clear
% draw homogeneous reaction case
% diffusion coefficient (cm^2/min)
D=7.4383e-6*60;
% reaction const (1/min)
K=0.00835;
% boundary conditions (mM)
f0=0.57;
fR=0;
% TNT molecular weight
MWtnt=227.16;
%density of TNT particle (g/cm^3)
Ptnt=1.654;
% time step
dt=1;
T=2000;
time=[0:dt:T]';
R=1;
RR=zeros(1,(T/dt)+1)';
Rm=0.1;
%step size
dr=(R-Rm)/40;
%x-grid points
r=[Rm:dr:R]';
r1=[Rm:dr:R-dr]';
% Matrix size
n=length(r);
% Set initial concentration
C=zeros(1,n)';
% Transform into dimensionless form
DB=D*dt/dr^2;
KB=K*dt;
%
%Set 2nd Diffusion coeff as a function of r
rn=r/R;
rn1=r1/R;
VB=(D./rn)*(dt/dr);
VB1=(D./rn1)*(dt/dr);
DFC1=DB/2*ones(n-1,1)-VB1/2;
DFC2=DB/2*ones(n-1,1)+VB1/2;
%
%construct the matrices Ap(+DB) and Am(-DB)
%and to solve Ap*C=Am*C+b
Ap=sparse(diag((1+DB+KB/2)*ones(n,1))-...
   diag(DFC2,1)-...
   diag(DFC1,-1));
Am=sparse(diag((1-DB-KB/2)*ones(n,1))+...
   diag(DFC2,1)+...
   diag(DFC1,-1));
F=zeros(1,(T/dt)+1)';
RR(1,1)=0.2;
```

```matlab
C(1,1)=f0;
%Boundary condition set as vector b
%for t=0:dt:T
b=VB.*[f0 zeros(1,n-2) fR]'+DB*[f0 zeros(1,n-2) fR]';
%C=Ap\(Am*C+b);
%figure(1),clf
%plot(r,C);hold on
for t=0:dt:T
    C=Ap\(Am*C+b);
%calculate the flux, and change the units
    F(t/dt+1,1)=D*(C(1,1)-C(2,1))/dr*MWtnt*1e-6;
%calculate the particle radius with flux
    if t<T & RR(t/dt+1,1)>F(t/dt+1,1)*dt/Ptnt
    RR(t/dt+2,1)=RR(t/dt+1,1)-F(t/dt+1,1)*dt/Ptnt;
    end
    if mod(t,10)==0
    plot(r,C)
    end
end
%hold off
%figure(2),clf;
%plot(time,F)
%end
figure(1), clf;
plot(time,RR);hold on
%
%draw the heterogeneous case
%Diffusion coefficient of alkaline OH (cm^2/min)
Doh=5.28e-5*60;
%concentration of OH in bulk solution (g/cm^3)
Coh=0.1105*0.001;
% Particle radius of TNT particle (cm)
Ro=0.2;
% reaction time and step
n=length(time);
%
r1=(Ro^2*ones(n,1)-6.6*Doh*Coh/Ptnt*time).^0.5;
plot(time,r1)
hold off
```

```matlab
%this script solves the TNT particle size versus time
%with heterogeneous surface reaction described in Levenspiel book
%enter parameter here
%Diffusion coefficient of alkaline OH (cm^2/min)
Doh=5.28e-5*60;
%viscosity of water (cm^2/s)
vis=0.01*60;
%density of TNT particle (g/cm^3)
Ptnt=1.654;
%concentration of OH in bulk solution (mM/L)
Coh=0.1105*0.01;
% reaction time and step
dt=5;
T=2000;
time=[0:dt:T]';
n=length(time);
t_mass=zeros(n);
Ptsize=[0.025,0.075,0.125,0.175,0.225]';
dist=[36,68,58,22,6]';
%
%case 1 --small particle without convection
figure(1);clf
for i=1:5
  plot(time,t_mass);hold on
  Ro=Ptsize(i);
  r1=real((Ro^2*ones(n,1)-6.6*Doh*Coh/Ptnt*time).^0.5);
  t_mass=4/3*pi*r1.^3*Ptnt*dist(i);
  plot(time,t_mass)
  axis([0 2000 0 0.9])
end
hold off
```

```
% This script is to solve shinking balls of TNT
% with outside diffusion and homogeneous reaction
% dc/dt= D/r^2[d(r^2(dc/dr))/dr]
% As time goes by, the ball radius decrease
% And the total mass will also changes
clear
% Enter parameter, those value is fixed
% D(diffusion coeff.)
D=7.4383e-6*60;
% K (reaction const)
K=0.00835;
% TNT molecular weight
MWtnt=227.16;
%density of TNT particle (g/cm^3)
Ptnt=1.654;
% boundary conditions
f0=0.57;
fR=0;
% time step
dt=10;
T=200000;
time=[0:dt:T]';
% Length setup, RR is particle size
Ptsize=[0.025,0.075,0.125,0.175,0.225]';
R=1;
RR=zeros(1,(T/dt)+1)';
% Particle size distrbution setup
dist=[36,68,58,22,6]';
t_mass=zeros(1,(T/dt)+1)';
%
%figure(1),clf
%plot(time,RR);hold on
figure(1),clf
plot(time,t_mass);hold on
for i=1:5
Rm=0.1;
%step size
dr=(R-Rm)/4;
%x-grid points
r=[Rm:dr:R]';
r1=[Rm:dr:R-dr]';
% Matrix size
n=length(r);
% Set initial concentration
C=zeros(1,n)';
C(1,1)=0.57;
% Transform into dimensionless form
DB=D*dt/dr^2;
KB=K*dt;
%
%Set 2nd Diffusion coeff as a function of r
rn=r/R;
rn1=r1/R;
VB=(D./rn)*(dt/dr);
```

```matlab
VB1=(D./rn1)*(dt/dr);
DFC1=DB/2*ones(n-1,1)-VB1/2;
DFC2=DB/2*ones(n-1,1)+VB1/2;
%
%construct the matrices Ap(+DB) and Am(-DB)
%and to solve Ap*C=Am*C+b
Ap=sparse(diag((1+DB+KB/2)*ones(n,1))-...
   diag(DFC2,1)-...
   diag(DFC1,-1));
Am=sparse(diag((1-DB-KB/2)*ones(n,1))+...
   diag(DFC2,1)+...
   diag(DFC1,-1));
%F=zeros(1,(T/dt)+1)';
RR(1,1)=Ptsize(i);
t_mass(1,1)=4/3*pi*RR(1,1)^3*dist(i)*Ptnt;
%Boundary condition set as vector b
for t=0:dt:T
b=VB.*[f0 zeros(1,n-2) fR]'+DB*[f0 zeros(1,n-2) fR]';
C=Ap\(Am*C+b);
%calculate the flux, and change the units
   F(t/dt+1,1)=D*(C(1,1)-C(2,1))/dr*MWtnt*1e-6;
% calculate the particle radius with flux
if t<T & RR(t/dt+1,1)>F(t/dt+1,1)*dt
   RR(t/dt+2,1)=RR(t/dt+1)-F(t/dt+1,1)*dt/Ptnt;
   t_mass(t/dt+2,1)=4/3*pi*RR(t/dt+2,1)^3*dist(i)*Ptnt;
end
end
%plot(time,RR)
plot(time,t_mass)
end
hold off
```

# REFERENCES

Anyanwu, N. N., Zirps, N. A., and Cerar, R. J., (1993). "Treatability Studies for Remediation of Explosives-Contaminated Goundwater." *Proceeding from Federal Environmental Restoration*, U. S. Army Environmental Center, 328-335, EDB94:065506.

Aris, R. (1975). *Mathematical Theory of Diffusion and Reaction in Permeable Catalysis*, Clarendon Press, Oxford, United Kingdom.

Bernasconi, C. F. (1971). "Kinetic and Spectral Study of Some Reactions of 2,4,6-Trinitrotoluene in Basic Solution. I Deprotonation and Janovsky Complex Formation". *Journal of Organic Chemistry*, Vol.36, No12, 1671-1679.

Blake, J. A., Evans, M. J. B., Russell, K. E., (1966). " Kinetics Studies of Proton Transfer from Phenol to Trinitrobenzyl Anion", *Canadian Journal of Chemistry*, Vol.44, 119-124.

Borse, G. J. (1997). *Numerical Methods with MATLAB : a resource for acientists and engineers*, PWS Publishing Company, Boston, MA.

Bradley, P. M. and Chapelle, F. H. (1995). "Factors Affecting Microbial, 2, 4, 6-Trinitrotoluene Mineralization in Comtaminated Soils" *Environmental Science & Technology*, Vol.29, 802-806.

Browning, G.L, Hack, J. J. and Swarztrauber, P.N. (1988). "A Comparison of Three Numerical for Solving Differential Equations of the Sphere", *Monthly Weather Review*, Vol. 107, 1058-1075.

Buncel, E., Russell, K. E. and Wood, J., (1968). "Hydrogen Exchange in 2,4,6-Trinitrotoluene", *Chemical Communications*, Vol.252, 252-253.

Chou, W-L, (1996). " The Study of Drug Delivery by Iontophoresis", Ph. D. Dissertation, Chemical Engineering Department, National Taiwan University.

Coulson J. M., Richardson, J.F., Backhurst, J. R. and Harker, J. H. (1991). *Chemical Engineering, vol.2 (Particle technology and separation processes)*, Pergamon Press, New York, 9-10.

Coulson J. M., Richardson, J.F., Backhurst, J. R. and Harker, J. H. (1991). *Chemical Engineering, vol.1 (Fluid flow, heat, transfer and mass transfer)*, Pergamon Press, New York, 625.

CRC (1997). *Handbook of Chemistry and Physics*. CRC Press, Boca Raton, FL.

Cussler, E. L. (1997). *Diffusion*, Cambridge, United Kingdom, 116-118, 22-24,375-389 (Ch15), 390-402, 129-134. 409-415.

Davis, M. E., (1984). *Numerical Methods & Modeling for Chemical Engineers*, John Wiley & Sons, NY.

Einstein, A., (1905). *Annalen der Physik*, Vol 17, 549.

Ferziger, J. H., (1981). *Numerical Methods for Engineering Application* , John Wiley & Sons, NY.

Fogler, H. S., (1992). *Elements of Chemical Reaction Engineering*, Prentice Hall, NJ.

Fraunhofer IITB – Aussenstelle fuer Prozessoptimerung Berlin, Analytisches Zentrum Berlin-Adlershof, and BC Berlin-Consult GmbH (1995). "Chemish-Biologisches Verfahren zur Entsorgung von TNT und TNT-haltigen Restoffen." Gemeinsamer Nericht zu den BMBF-Forschungsvorhaben.

Gallagher, H. G., Roberts, K. J., Sherwood, J. N. and Smith, A. L, (1997). "A theoretical examination of the molecular packing, intermolecular bonding and Crystal morphology of 2, 4, 6-trinitrotoluene in relation to polymorphic structural stability." *J. Mater. Chem*. Vol.7, No2, 229-235.

Hantzsch A, and H, Kissel (1899). *Berlin Springer Verlag*, Vol. 32.

Helimann, H. M. Wiesmann, U., and Stenstrom, M. K. (1996). Kinetics of the Aqueous Homogeneous Alkaline Hydrolysis of High Explosives RDX and HMX. *Environmental Science & Technology*, Vol. 30, No5, 1485-1492.

Hammersley, V. L. (1975). "Historical and Experimental Studies of Alkali and Trinitrotoluene Reaction", Naval Weapons Support Center, Report WQEC/C-75-192.

Jones, W., Mahannah, J., Sommerer, S. and Kitchens, J. (1982). "Engineering and Development Support of General Decon Technology for the US Army's Installation Restoration Program" Task 5 Facility Decontamination, Atlantic Research Corporation, Alexandia, VA, Report to the US Army Toxic and Hazardous Materials Agency.

Kaplan, D. L. and Kaplan, A. M., (1982). "Thermophilic Biotransformations of 2, 4, 6-Trinitrotoluene under Simulated Composting Conditions." *Applied and Environmental Microbiology*, Vol.44, No2, 757-760.

Levenspiel, O. (1972). *Chemical Raction Egineering*, John Wiley & Sons Inc, Canada, 358-359, 368-371.

Mackay, D. and Paterson, S., (1981). "Calculating Fugacity" *Environmental Science & Technology*, Vol.15. No.9, 1006-1014.

Major, M. A. and Amos, J. C., (1992). "Incineration of Explosive Contaminated Soil as a means of Site Remediation" U. S. Army Biomedical Research & Development Laboratory, Fort Detrick AD-A258 757.

McCall, P. J., Swann, R. L. and Laskowski, D. A., (1983). " Partition Models for Equilibrium Distribution of Chemicals in Environmental Compartments", Fate of Chemicals in the Environment, American Chemical Society, 107-122.

Ojha, S. (1997). "Treatment and Biodegradation of the High Explosive 2,4,6-Trinitrotoluene (TNT): A Literature Review", Master Thesis, Civil and Environmental Department, UCLA.

Okamoto, Y., Chou, E. J. and Croce, M., (1978). "Application of Form Separation of Aqueous Solutions of Trinitrotoluene (TNT) Part II. Removal of Organic Explosives with Surfacetants", U. S. Army Armament Research and Development Command, ARLCD-78020.

Okamoto, Y. and Wang, J., (1977). "Micellar Effects on the Reaction of 2, 4,6-trinitrotoluene with Amines", *Journal of Organic Chemistry*, Vol.42, No7, 1261-1262.

Osmon J. L. and Klausmeier, R. E., (1972). "Microbial Drgradation of Explosives", *Dev. Ind. Microbiology*, Vol.14, 247-252.

Pärt-Enander, E. and Sjöberg, A. (1999). *The Matlab 5 Handbook*, Addison-Wesley, United Kindom.

Priestley, D. (1998). "Alkaline Hydrolysis of TNT", Master Thesis, Civil and Environmental Department, UCLA.

Riemer, B., (1995). "Theoretische Betrachtungen moeglicher Reaktionswege bei der Desenbiliserung von TNT unter alkalishen Bedingungen", *TUV-akademie Berlin-Brandenburg*, Gmbh, Potsdam, Germany.

Ro, K. S., Venogopal, A., Adrian, D., Constan, D., Qaisi, D., Valsaraj, T., Thibodeaux, L. J. and Roy, D., (1996). "Optimizing of an Aerobic Polishing Stage to Complet the Anaerobic Treatment of Munitions-Contaminated Soils" *Environmental Science & Technology*, Vol.30, No.6, 2021-2026.

Rowley. R. L. (1994). *Statisical Mechanics for Thermophysical Property Calculations*, Prentice Hall, New Jersey, 294-297; 215-222.

Saupe, A., Heinze, L., Simmert, J., Dahn, A. and Koehler, P. (1996). " Das Hydrobio-Verfahren zur Sanierung von TNT-Altlasten", *TerraTech* 3, 58-60.

Schwarzenbach, R. P., Gschwend, P. M. and Imboden, D. M. (1993). *Environmental Organic Chemistry*, John Wiley & Sons Inc, 194-200.

Spontarelli, T., Buntain, G. A., Sanchez, J. A. and Benzinger, T. M. (1993). "Destruction of Waste Energetic Material Using Base Hydrolysis", Proceedings of the 1993 Incineration Conference.

Spontarelli, T., Sanchez, J., (1993). "Remediation of Explosives-Abstract", *Emerging Technologies in Hazardous Waste Management VI*, Vol.2, 171.

Stenstrom, M. K. and Song, S. S. (1991). "Effects of Oxygen Transfer Limitation on Nitrification in the Activated Sludge Process", *Research Journal of the Water Pollution Control Federation*, Vol.63, No3, 208-219.

Stokes, G. G., (1850). *Transactions of the Cambridge Philosophical Society*, Vol 9, 8.

Swarztrauber, P. N., Willamson, D. L. and Drake, J. B. (1996). "The Cartesian Method for Solving Partical Differential Equations in Spherical Geometry", *Dynamics of Atmospheres and Oceans*, Vol.27, 679-706

Tsai, T. S., (1991). "Biotreatment of Red Water – a Hazardous Waste Stream form Explosive Manufacture – with Fungal System". *Hazardous Waste & Hazardous Materials*, Vol.8, No3, 231-244.

Urbanski, T (1964). *Chemistry and Technology of Explosives*, Vol.1., Pergamon Press, New, York, 290-310.

US EPA (1995), *Ex-situ Anaerobic bioremediation Technology : TNT*, Science Applications International Corp, San Diego, EPA/540/R-95/529A, 1-9.

Yinon, J. (1990) Toxicity and Metabolism of Explosives, CRC Press inc, Boco Raton, Fl.

US Department of Health and Human Services (1995). "Toxilogical profile for 2,4,6-trinitrotoluene", Sciences International, Inc, 1-6, 87-113.

Zappi, M., Toro, E., Guimbellot, D. and Ragan, F. (1994). "Slurry Oxidation of Trinitrotoluen Contaminated Soil- Abstract", *Emerging Technologies in Hazardous Waste Management VI*, Vol.1, 301.